Int. J. Dynam. Control (2018) 6:122–139
https://doi.org/10.1007/s40435-017-0310-1

A patchy model for the transmission dynamics of tuberculosis in sub-Saharan Africa

D. P. Moualeu[1] · S. Bowong[2,4] · B. Tsanou[3] · A. Temgoua[2]

Received: 6 August 2016 / Revised: 25 January 2017 / Accepted: 2 February 2017 / Published online: 24 February 2017

Abstract Tuberculosis (TB) spreads through contact between a susceptible person and smear positive pulmonary TB case (TPM+). The spread of TB is highly dependent on people migration between cities or regions that may have different contact rates and different environmental parameters, leading to different disease spread speed in the population. In this work, a metapopulation model, i.e., networks of populations connected by migratory flows, which overcomes the assumption of homogeneous mixing between different regions was constructed. The TB model was combined to a simple demographic structure for the population living in a multi-patch environment (cities, towns, regions or countries). The model consist of a system of differential equations coupling TB epidemic at different strength and mobility between the patches. Constant recruitment rate, slow and fast progression to the disease, effective chemoprophylaxis, diagnostic and treatment are taken into account to make the model including the reality of people in the sub-Saharan African countries. The basic reproduction number ($\mathcal{R}_0$) was computed and it was demonstrated that the disease-free equilibrium is globally asymptotically stable if $\mathcal{R}_0 < 1$. When $\mathcal{R}_0 > 1$, the disease-free equilibrium is unstable and there exists one endemic equilibrium. Moreover, the impact of increasing migration rate between patches on the TB spread was quantified using numerical implementation of the model. Using an example on 15 inter-connected patches on the same road, we demonstrated that most people was most likely to get infected if the disease starts in a patch in the middle than in border patches.

Keywords Nonlinear dynamical systems · Epidemiological models · Meta-population · Tuberculosis · Stability

Mathematics Subject Classification 34A34 · 34D23 · 34D40 · 92D30

1 Introduction

Tuberculosis (abbreviated as TB for tubercle bacillus) is a common deadly infectious disease caused mainly by the *Mycobacterium tuberculosis* (MTB) that primarily attacks the lungs (pulmonary TB). TB can also affect the central nervous system, the circulatory system, the genital-urinary system, bones, joints and even the skin. MTB spreads mostly through contact with active pulmonary TB persons, although [1,2] and not from latently infected persons. MTB transmission depends on the number of infectious droplets expelled by a carrier, the effectiveness of ventilation, duration of the exposure and virulence of the MTB strain [1–5]. The transmission chain can therefore be broken by isolating patients with active disease and starting effective anti-tuberculosis therapy [1–5]. Nowadays, about 95% of the estimated 8 million new TB cases occurring each year are in developing

✉ S. Bowong
sbowong@gmail.com

1 Institute for Horticultural Production Systems, Vegetable Systems Modelling Section, Faculty of Natural Sciences, Leibniz Universität Hannover, Herrenhäuser Str. 2, 30419 Hannover, Germany

2 Department of Mathematics and Computer Science, Faculty of Science, University of Douala, PO Box 24157, Douala, Cameroon

3 Department of Mathematics and Computer Science, Faculty of Science, University of Dschang, PO Box 47, Dschang, Cameroon

4 UMI 209 IRD/UPMC UMMISCO, Bondy-France and GRIMCAPE-Cameroon, The African Center of Excellence in Information and Communication Technologies (CETIC), University of Yaounde 1, Yaounde, Cameroon

countries, where 80% occur among people between the ages of 15–59 years [1], although several strategies for TB control propagation are implemented. The reason of these fails might on the heterogeneity of the countries and difficulties to access to treatment in some places. In fact, heterogeneity plays an important role in many infectious disease processes. For instance, spatial heterogeneity is a strong determinant of host-parasite relationships. In modeling spatial or geographic effects on the spread of a disease, a distinction is usually made between diffusion and dispersal models. In diffusion models, spread is made to immediately adjacent zones, hence the phenomenon of traveling waves can appear. These models traditionally use partial differential equations (PDE). However, there are some important situations that cannot be modeled by PDE. This is the case when the space considered is discrete. For example, when sparsely populated regions have to be considered, the human population is located in patches. The organization of human-hosts into well-defined social units such as families, villages or cities, are good examples of patches. Another example arises in the study of the human African Trypanosomiasis. For situations where human can travel a long distance in a short period of time, dispersal models are more appropriate to capture heterogeneity.

When considering dispersal models, there is an approach based on the metapopulation concept. The population is subdivided into a number of discrete patches which are supposed to be well mixed. Then in each patch, the population is subdivided into compartments corresponding to different epidemic status. This leads to a multi-compartment system. At this point two formulations are possible. The first one assumes that an infective in one patch can infect susceptible individuals in another patch. This assumption gives rise to a family of models which have been well studied [6–8]. The seminal model of [7] is the prototype of such systems. This formulation assumes that there is a spatial coupling between patches, but that individuals (vectors or hosts) do not migrate between patches. They make short 'visits' from their home patches to other patches. A number of theoretical studies have focused on the mathematical modelling of the spread of infectious diseases in heterogeneous complex metapopulations. Sattenspiel and Dietz [9] introduced a SIR epidemic model with population mobility. A two-patch model of trypanosomiasis is considered in [10] to explore control strategies through numerical simulations. Wang and Mulone [11] have computed the basic reproduction ratio $\mathcal{R}_0$ for a SIS model, with "true action mass" on two patches. In [12], Arino and van den Driessche computed the basic reproduction number $\mathcal{R}_0$ for a SEIRS model with mass action and constant population on n patches. Fromont et al. [13] studied a SIR model with density-dependent dynamics on n patches and applied this model to the Feline leukemia virus infection on cats. A SIS model with "pseudo mass action" and vital dynamics on n patches was considered in [14]. They computed the basic reproduction number $\mathcal{R}_0$ and proved the global stability of the disease-free equilibrium (DFE) whenever $\mathcal{R}_0 < 1$ when infective and susceptible individuals have the same dispersal rate. They have also proved the permanence of the disease when $\mathcal{R}_0 > 1$. A local study of a SIR model on n patches has been studied by Lloyd and Jansen [15]. Using the framework of Arino and van den Driessche [11], Ruan et al. [16] studied the global spread of SARS. They computed the $\mathcal{R}_0$. Arino et al. [17] considered SEIRS multi-species epidemic models on n patches with migration, which could be used as vector-hosts models. They computed $\mathcal{R}_0$ and obtained by simulation, epidemic waves on a ring of patches. In [12] a review on epidemiological metapopulation models was given. A SIS model on n patches, with true action mass and with migration, where infective and susceptible individuals can have different migration rates has been studied by Allen et al. [18]. They computed the R_0, proved the global asymptotic stability of the DFE when $\mathcal{R}_0 < 1$ and have shown that there exists a unique endemic equilibrium when $\mathcal{R}_0 > 1$. All the previous examples, except those in [12,17,19] have considered directly transmitted diseases. More recently in [20], the authors studied a SEI model of TB on two patches, with true action mass and different migration rates of susceptible and infective individuals. However, a number of theoretical studies was carried out on the mathematical modelling of TB transmission dynamics [21–29]. However, only a few of these studies have considered the mathematical modelling of the spread of TB in heterogeneous complex metapopulations.

In this paper, motivated by the usefulness of and the current investigation on the spread of infectious diseases on heterogeneous populations, we intend to systematically investigate the analysis of the spread of tuberculosis in sub-Saharan Africa in the modelling framework. The aim of this work is to link the cities, taking into account human movements, that could explain the spread of tuberculosis (TB). For instance, in sub-Saharan Africa, many people move a lot from place to place to go from Home to work and back or to visit family or friends. Moreover, it is well known that due to the symptoms of the disease, infectious were not able to move. Thus, in our model, we intend to take into account limitation movements of infectious and show that it can have an impact in the spread and the force of the infection.

We consider the spread of TB on complex metapopulations, i.e., networks of populations connected by migratory flows. Each population within the metapopulation is composed of subpopulations of each of the various epidemiological status. Ordinary differential equations (ODE) are used to model the local interactions of these subpopulations within each compartment as well as the migration of subpopulations between adjacent compartments. Here, a patch may represent a city, a town, a region or a country, and population movements between patches may be justified by

the migration or travel among patches. We distinguish n patches. For overall patches, we divided the infective class into two subgroups with different properties: (i) diagnosed infectious and (ii) undiagnosed infectious. Based on the fact that diagnosed infected are educated about the disease and its infectivity, and undiagnosed in many villages or regions in Africa do not know their TB-status due to the absence of hospital in rural areas, education, mentalities and so on, we assume that the transmission of the infection from diagnosed infectious to susceptible individuals is frequency-dependent (standard incidence), while the transmission of the infection from undiagnosed infectious to susceptible individuals is density-dependent (simple mass action), i.e., non-limited. We compute the disease-free equilibrium and the basic reproduction number $\mathcal{R}_0$. We show that the disease-free equilibrium is globally asymptotically stable when $\mathcal{R}_0 < 1$. Using implicit function theorem, we show that there exist a unique endemic equilibrium in a small neighborhood of the isolated endemic equilibrium for weak (small) migration rates. Numerical studies are presented to validate analytical results. Comparing to existing results [30], our work differs from these studies in that our model in addition to undiagnosed infectious, our model also considers the natural recovery and traditional medicine (practiced in sub-Saharan Africa). It is our view fact that this study represents the first work that provides an in-depth the spread of TB on complex metapopulation networks in sub-Saharan Africa which take into account both standard and mass action incidences in the force of the infection.

2 Model construction

2.1 Migration model

The transfer rate from patch i to patch j, for $i \neq j$, is denoted by $m_{ji} \geq 0$. It is assumed that the infection and death due to the disease do not occur during the travel, but only in different patches. Let $N_i(t)$ be the total Human population in patch i. Then, for $i = 1, \ldots, n$, the dynamics of $N_i(t)$ is given by

$$\dot{N}_i = \pi_i - \mu_i N_i + \sum_{j \neq i}^{n} m_{ij} N_j - N_i \sum_{j \neq i}^{n} m_{ji}, \tag{1}$$

where μ_i denotes the mortality rate of individuals in patch i and π_i the recruitment inside the population of patch i.

System (1) can be written in the following compact form for all patches together:

$$\dot{N} = \pi - \text{diag}(\mu)N + \mathcal{M}N, \tag{2}$$

where $N = (N_1, \ldots, N_n)^T$, $\pi = (\pi_1, \ldots, \pi_n)^T$, $\mu = (\mu_1, \ldots, \mu_n)^T$, the superscript T denoting the transpose, the matrix $\mathcal{M}$ is defined by $\mathcal{M}(i, j) = m_{ij}$ for $i \neq j$ and $\mathcal{M}(i, i) = -\sum_{j=1}^{n} m_{ji}$ and diag(μ) the diagonal matrix with μ_i as its (i, i) entry.

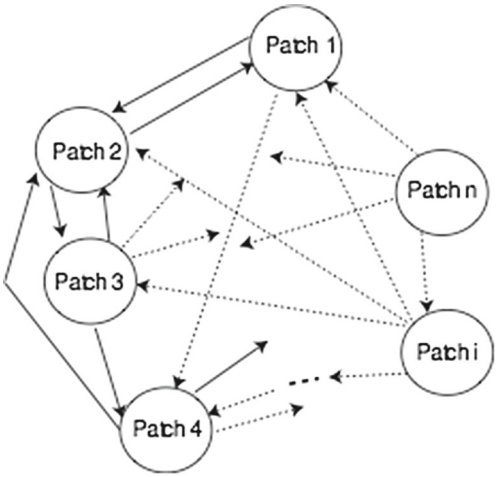

Fig. 1 A general n-patches model for the transmission of TB between n cities. *Solid line* stands for strong connection between cities, while the *dotted line* represent "weak" connections

Model (2) does not keep track of where an individual usually resides, but just considers where he is at time t. The migration model flowchart is presented in Fig. 1.

2.2 TB metapopulation model

In each sub-population, based on epidemiological status, the basic model included classes of susceptible, infected, infective and recovered individuals, and hence are known as SEIR (Susceptible–Infected–Infective–Recovered) models [31–33]. The infective class is divided into two subclasses with different properties: diagnosed and undiagnosed infectious. At time (t), each individual is assumed to be in one of the following states: susceptible, latently infected (exposed to TB but not infectious), diagnosed infectious (active TB confirmed after a sputum examination in the hospital), undiagnosed infectious (have an active TB not diagnosed in a sputum examination in the hospital), and recovered individuals (cured after a therapy of treatment). For a patch i, states variables are denoted by S_i, E_i, I_i, J_i and R_i, respectively. The model is based on the following assumptions.

Diagnosed infected population transmit the disease to a susceptible with a frequency-dependent (i.e., limited) force of infection, while undiagnosed infectious have a density-dependent (i.e., non-limited) force of infection [34–36].

The rate constant for non-disease related death is μ_i, thus, $1/\mu_i$ is the average lifetime. Diagnosed and undiagnosed infectious have addition death rates due to disease with rates d_i and δ_i, respectively. Transmission of MTB occurs after adequate contacts between susceptible, diagnosed and undi-

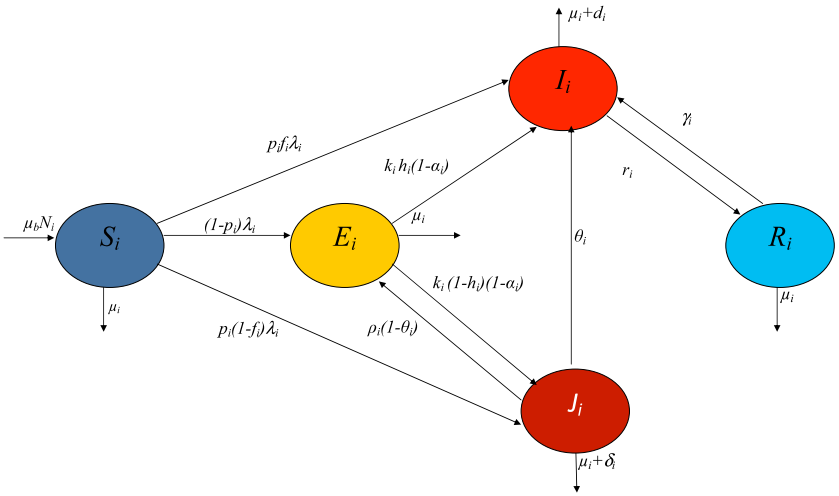

Fig. 2 Flow diagram for the dynamics transmission of tuberculosis in patch i where $\lambda_i = \beta_i \left(\frac{I_i}{N_i} + \varepsilon_i J_i \right)$ is the force of the infection

agnosed infectious. Then, susceptible individuals of patch i acquire TB infection from individuals with active TB at rate λ_i, given by

$$\lambda_i = \beta_i \frac{I_i}{N_i} + \varepsilon_i \beta_i J_i, \tag{3}$$

where β_i is the effective contact rate of diagnosed and undiagnosed infectious that is sufficient to transmit the infection to susceptible individuals in patch i, and the parameter ε_i accounts the higher infectiousness of undiagnosed infections with respect to diagnosed infections. Upon adequate contacts with active TB, a susceptible individual becomes infected but not yet infectious. A proportion p_i of the latently-infected individuals develops a fast active TB and the remainder $(1 - p_i)$ develops a latent TB and enters the latent class E_i. Among latently-infected individuals who develop a fast active TB, a proportion f_i is assumed to undergo a fast progression directly to the diagnosed infectious class I_i, while the remainder $(1 - f_i)$ enter the undiagnosed infectious class J_i.

Once latently infected with MTB, an individual will remain so for life unless reactivation occurs. Latently infected individuals are assumed to acquire some immunity as a result of infection, which reduces the risk of subsequent infection but does not fully prevent it. Once latently infected, an individual can follow a chemoprophylaxis. We assume that chemoprophylaxis of latently infected individuals reduces their reactivation. We denote by α_i the rate of chemoprophylaxis of latently-infected individuals in patch i. Thus, $\alpha_i E_i$ is the number of latently-infected individuals who received chemoprophylaxis in patch i. Due to endogenous reactivation, a proportion $1 - \alpha_i$ of latently infected individuals who did not received effective chemoprophylaxis becomes infectious at rate k_i. Among latently infected individuals which become infectious, a proportion h_i of them is diagnosed and treated, while the remaining $1 - h_i$ is not diagnosed and enter the class of undiagnosed infectious J_i. It is assumed that after many attempts to treat the disease, some undiagnosed infectious will decide to to to the hospital at a constant rate θ_i. Also, due to their own immunity, traditional medicine and drugs bought in the street (practiced in sub-Saharan Africa), a proportion $1 - \theta_i$ of undiagnosed infectious who do not go to the hospital can spontaneously recover from the disease at a constant rate ρ_i and enter the latent class E_i. After a therapy of treatment, diagnosed infectious might be declared cured of the disease and enter the recovered class R_i at rate r_i. As suggested by Styblo et al. [37], recovered individuals can only have partial immunity. Hence, they can undergo a reactivation of the disease and move to the class I_i at rate γ_i [34–36].

This description is summarized in the flow diagram shown in Fig. 2.

This yields the following differential equations for $i = 1, \ldots, n$:

$$\begin{cases} \dot{S}_i = \pi_i - \lambda_i S_i - \mu_i S_i + \sum_{j=1}^{n} m_{ij} S_j - S_i \sum_{j=1}^{n} m_{ji}, \\ \dot{E}_i = (1 - p_i)\lambda_i S_i + \rho_i (1 - \theta_i) J_i - A_{E_i} E_i \\ \qquad + \sum_{j=1}^{n} m_{ij} E_j - E_i \sum_{j=1}^{n} m_{ji}, \\ \dot{I}_i = p_i f_i \lambda_i S_i + \theta_i J_i + \gamma_i R_i + h_i (1 - \alpha_i) k_i E_i \\ \qquad - A_{I_i} I_i + \eta \left(\sum_{j=1}^{n} m_{ij} I_j - I_i \sum_{j=1}^{n} m_{ji} \right), \\ \dot{J}_i = p_i (1 - f_i)\lambda_i S_i + (1 - h_i)(1 - \alpha_i) k_i E_i \\ \qquad - A_{J_i} J_i + \eta \left(\sum_{j=1}^{n} m_{ij} J_j - J_i \sum_{j \neq i}^{n} m_{ji} \right), \\ \dot{R}_i = r_i I_i - A_{R_i} R_i + \sum_{j=1}^{n} m_{ij} R_j - R_i \sum_{j=1}^{n} m_{ji}, \end{cases} \tag{4}$$

where m_{ij} are the migration rates from patch j to patch i (with $i \neq j$),

$$A_{E_i} = \mu_i + k_i(1-\alpha_i), \qquad A_{I_i} = \mu_i + d_i + r_i,$$
$$A_{J_i} = \mu_i + \delta_i + \theta_i + \rho_i(1-\theta_i) \quad \text{and} \quad A_{R_i} = \gamma_i + \mu_i.$$

For $i = 1, \ldots, n$, the dynamics of the total population becomes

$$\begin{aligned}\dot{N}_i = \pi_i - \mu_i N_i + \sum_{j=1}^{n} m_{ij}(S_j + E_j + R_j + \eta(I_j + J_j)) \\ - (S_i + E_i + R_i + \eta(I_i + J_i)) \sum_{j=1}^{n} m_{ji} \\ - (\delta_i J_i + d_i I_i).\end{aligned} \tag{5}$$

Setting $H(t) = \sum_{i=1}^{n} N_i(t)$, the dynamics of the total population is

$$\dot{H} = \Pi - \sum_{i=1}^{n} \mu_i N_i - \sum_{i=1}^{n} (\delta_i J_i + d_i I_i), \tag{6}$$

where $\Pi = \sum_{i=1}^{n} \pi_i$.

Setting $S = (S_1, \ldots, S_n)^T$, $E = (E_1, \ldots, E_n)^T$, $I = (I_1, \ldots, I_n)^T$, $J = (J_1, \ldots, J_n)^T$ and $R = (R_1, \ldots, R_n)^T$, system (4) becomes:

$$\begin{cases} \dot{S} = \pi - \text{diag}(\lambda)S - \text{diag}(\mu)S + \mathcal{M}S, \\ \dot{E} = \text{diag}((\mathbb{1} - p)\cdot\lambda)S + \text{diag}(\rho\cdot(\mathbb{1}-\theta))J \\ \quad - \text{diag}(A_E)E + \mathcal{M}E, \\ \dot{I} = \text{diag}((p\cdot f)\cdot\lambda)S + \text{diag}(\theta)J + \text{diag}(\gamma)R \\ \quad + \text{diag}(h.(\mathbb{1}-\alpha).k)E - \text{diag}(A_I)I + \eta\mathcal{M}I, \\ \dot{J} = \text{diag}((p\cdot(\mathbb{1}-f)\cdot\lambda)S + \text{diag}(\mathbb{1}-h)\cdot(\mathbb{1}-\alpha)\cdot k)E \\ \quad - \text{diag}(A_J)J + \eta\mathcal{M}J, \\ \dot{R} = \text{diag}(r)I - \text{diag}(A_R)R + \mathcal{M}R, \end{cases} \tag{7}$$

where $\pi = (\pi_1, \ldots, \pi_n)^T$, $\lambda = (\lambda_1, \ldots, \lambda_n)^T$, $\mu = (\mu_1, \ldots, \mu_n)^T$, $p = (p_1, \ldots, p_n)^T$, $\rho = (\rho_1, \ldots, \rho_n)^T$, $\theta = (\theta_1, \ldots, \theta_n)^T$, $f = (f_1, \ldots, f_n)^T$, $\alpha = (\alpha_1, \ldots, \alpha_n)^T$, $A_E = (A_{E_1}, \ldots, A_{E_n})^T$, $A_I = (A_{I_1}, \ldots, A_{I_n})^T$, $A_J = (A_{J_1}, \ldots, A_{J_n})^T$, $A_R = (A_{R_1}, \ldots, A_{R_n})^T$, $k = (k_1, \ldots, k_n)^T$, $h = (h_1, \ldots, h_n)^T$ and $r = (r_1, \ldots, r_n)^T$, $\mathbb{1} = (1, \ldots, 1)^T$.

In system (7), the notation "$a.b$", where a and b are vectors with the same dimension denotes, the component-wise vector multiplication, $\mathcal{M}$ is defined as in Eq. (2) and $N = S + E + I + J + R$ is the vector-size of the total population.

Adding all equations in system (7) gave

$$\begin{aligned}\dot{N} = \pi - \text{diag}(\mu)N + \mathcal{M}[S + E + R + \eta(I + J)] \\ - [\text{diag}(\delta)J + \text{diag}(d)I],\end{aligned} \tag{8}$$

where $\mathcal{M}$ was defined in Eq. (2)

System (7) was written in a more compact form as:

$$\begin{cases} \dot{x} = \pi - \text{diag}(\lambda)x + (\mathcal{M} - \text{diag}(\mu))x, \\ \dot{y} = B\text{diag}(\lambda)x + V_y\, y, \end{cases} \tag{9}$$

where $x = S \in \mathbb{R}_+^n$ stands for the susceptible individuals and $y = (E, I, J, R)^T \in \mathbb{R}_+^{4n}$ was the vector representing the state of infected individuals (latently infected, diagnosed and undiagnosed infectious and recovered individuals).

$$B = (\text{diag}(\mathbb{1} - p), \text{diag}(p\cdot f), \text{diag}(p\cdot(\mathbb{1} - f)), 0)^T, \tag{10}$$

is a $(4n \times n)$ block matrix, and V_y is a constant matrix, given by

$$V_y = \begin{bmatrix} \mathcal{M} - \text{diag}(A_E) & 0 & \text{diag}(\rho.(\mathbb{1}-\theta)) & 0 \\ \text{diag}(k\cdot h\cdot(\mathbb{1}-\alpha)) & \eta\mathcal{M} - \text{diag}(A_I) & \text{diag}(\theta) & \text{diag}(\gamma) \\ \text{diag}(k\cdot(\mathbb{1}-h)\cdot(\mathbb{1}-\alpha)) & 0 & \eta\mathcal{M} - \text{diag}(A_J) & 0 \\ 0 & \text{diag}(r) & 0 & \mathcal{M} - \text{diag}(A_R) \end{bmatrix},$$

with A_E, A_I, A_J and A_R defined as in Eq. (4).

V_y and $[\mathcal{M} - \text{diag}(\mu)]$ are Metzler matrices since their off-diagonal entries are non-negative [38,39]. It follows that they are stable and invertible matrices. The following result can be applied for V_y and $[\text{diag}(\mu) - \mathcal{M})]^{-1}$.

Lemma 1 *The matrix V_y and $[diag(\mu) - \mathcal{M})]^{-1}$ are stable matrix. All the eigenvalues of V_y and $[diag(\mu) - \mathcal{M})]^{-1}$ have negative real parts.*

Proof Note that $V_y = [V_y(i, j)]_{i,j=1,\ldots,n}$, is a diagonal column dominant matrix. Indeed, for $i = 1, \ldots, n$, one has that

$$\begin{aligned}\sum_{j\neq i}^{4n} \mid V_y(i, j) \mid &= k_i(1-\alpha_i) + \sum_{j=1}^{n} m_{ij} \\ &< A_{E_i} + \sum_{j=1}^{n} m_{ij} \\ &= \mid -A_{E_i} - \sum_{j=1}^{n} m_{ij} \mid = \mid V_y(i, i) \mid .\end{aligned} \tag{11}$$

Similarly for $i = n+1, \ldots, 2n$, one has

$$\begin{aligned}\sum_{j\neq i}^{4n} \mid V_y(i, j) \mid &= r_i + \sum_{j=1}^{n} \eta\, m_{ij} < A_{I_i} + \sum_{j=1}^{n} \eta\, m_{ij} \\ &= \mid -A_{I_i} - \sum_{j=1}^{n} \eta\, m_{ij} \mid = \mid V_y(i, i) \mid .\end{aligned} \tag{12}$$

Also, for $i = 2n+1, \ldots, 3n$,

$$\begin{aligned}\sum_{j\neq i}^{4n} \mid V_y(i,j) \mid &= \theta_i + \rho_i(1-\theta_i) + \sum_{j=1}^{n} \eta\, m_{ij} \\ &< A_{J_i} + \sum_{j=1}^{n} \eta\, m_{ij} \\ &= \mid -A_{J_i} - \sum_{j=1}^{n} \eta\, m_{ij} \mid = \mid V_y(i,i) \mid . \quad (13)\end{aligned}$$

Similarly for $i = 3n+1, \ldots, 4n$, one obtains

$$\begin{aligned}\sum_{j\neq i}^{4n} V_y(i,j) &= \gamma_i + \sum_{j=1}^{n} m_{ij} < A_{R_i} + \sum_{j=1}^{n} m_{ji} \\ &= \mid -A_{R_i} - \sum_{j=1}^{n} m_{ji} \mid = \mid V_y(i,i) \mid, \quad (14)\end{aligned}$$

and

$$\begin{aligned}\sum_{j\neq i}^{4n} V_y(i,j) &= \gamma_i + \sum_{j=1}^{n} m_{ij} < A_{R_i} + \sum_{j=1}^{n} m_{ji} \\ &= \mid -A_{R_i} - \sum_{j=1}^{n} m_{ji} \mid = \mid V_y(i,i) \mid . \quad (15)\end{aligned}$$

By Gershgorin circle theorem [30], we know that each eigenvalue of V_y lies in the union of the following circles

$$\mid z + V_y(i,i) \mid \leq \sum_{j\neq i}^{4n} \mid V_y(j,i) \mid, \quad i = 1, \ldots, n. \quad (16)$$

Then, Eqs. (15) and (11)–(14) imply that the real part of each eigenvalue of V_y is negative. Hence, V_y is stable and invertible. Moreover, since V_y is a M-matrix (opposite of a Metzler matrix), it is known from [38] that $-V_y^{-1}$ is nonnegative. This concludes the proof. □

Remark 1 The same proof can be used to show that the M-matrix $[\mathrm{diag}(\mu) - \mathcal{M}]$ is invertible and that $[\mathrm{diag}(\mu) - \mathcal{M}]^{-1}$ is nonnegative.

2.3 Basic properties of the model

Following results are straigthforward for model 9:

Lemma 2 1. *The nonnegative orthant $\mathbb{R}^{5n}_+$ is positively invariant for system (9).*
2. *Each non-negative solution of system (4) is bounded by* $\max\left(\frac{\Pi}{\mu_{min}}, H(0)\right)$ *where* $\Pi = \sum_{i=1}^{n} \pi_i$ *and* $\mu_{min} = \min_{1\leq i\leq n}(\mu_i)$.

From the Susceptible population equation,

$$\dot{S} \leq \pi - [\mathrm{diag}(\mu) - \mathcal{M}]S.$$

One can easily prove that

$$\limsup_{t\to\infty} S(t) \leq S^0, \quad (17)$$

where $S^0 = -[\mathcal{M} - \mathrm{diag}(\mu)]^{-1}\pi$. Then, the following result is straightforward.

Corollary 1 *The set*

$$\Omega = \left\{ (S(t), E(t), (t), J(t), R(t)) \in \mathbb{R}^{5n}_+,\ S(t) \leq S^0, \right.$$
$$\left. H(t) \leq \max\left(\frac{\Pi}{\mu_{min}}, H(0)\right)\right\}, \quad (18)$$

is a compact forward invariant and absorbing set for system (7).

It can be easily shown that Ω, is positively-invariant under the flow induced by model system (7). Since the solutions are bounded, the usual existence uniqueness and continuation results hold for the system (7) for all $t \geq 0$. Hence, model system (7) is well posed mathematically and epidemiologically and it is sufficient to consider the dynamics of the flow generated by model system (7) in Ω. Therefore, the following result follows.

Theorem 1 *For every non-zero, non-negative initial values, solutions of system (4) exist for all times.*

Proof Local existence of solutions follows from standard arguments since the right-hand side of system (4) is locally Lipschitz continuous. Global existence follows from a priori bounds. □

3 Main results

3.1 The disease-free equilibrium (DFE)

We consider system (7). Let $P_0 = (S^0, E^0, I^0, J^0, R^0)$ be that disease free equilibrium. Then, by definition one has $I^0 = J^0 = 0$. Thus, $\lambda = 0$, and system (7) at the DFE P_0 is

$$\begin{cases} 0 = \pi - \mathrm{diag}(\mu)S^0 + \mathcal{M}S^0, \\ 0 = -\mathrm{diag}(A_E)E^0 + \mathcal{M}E^0, \\ 0 = \mathrm{diag}(\gamma)R^0 + \mathrm{diag}(h\cdot(\mathbb{1}-\alpha)\cdot k)E^0, \\ 0 = \mathrm{diag}((\mathbb{1}-h)\cdot(\mathbb{1}-\alpha)\cdot k)E^0, \\ 0 = [\mathrm{diag}(A_R) - \mathcal{M}]R^0. \end{cases} \quad (19)$$

From system (19), it is straightforward to see that $E^0 = R^0 = 0$ since the matrices $\mathrm{diag}((\mathbb{1}-h)\cdot(\mathbb{1}-\alpha).k)$ and

$[\text{diag}(A_R) - \mathcal{M}]$ are invertible (see Theorem 1). It remain to determine S^0. To do so, adding all equations in (19) yield

$$[\mathcal{M} - \text{diag}(\mu)]S^0 = -\pi. \tag{20}$$

Now, using the fact that $[\mathcal{M} - \text{diag}(\mu)]$ is inversible and $[\mathcal{M} - \text{diag}(\mu)]^{-1}$ is nonnegative, one has that

$$S^0 = -[\mathcal{M} - \text{diag}(\mu)]^{-1}\pi. \tag{21}$$

Finally, we have proved the following result.

Lemma 3 *The disease-free equilibrium of model system (7) is* $P_0 = (S^0, 0, 0, 0)$ *where* S^0 *is defined as in Eq. (21).*

3.2 The basic reproduction number

We compute the basic reproduction number $\mathcal{R}_0$, using the next generation approach, developed in van den Driessche and Watmough [40]. Using the notations in [40] and the second equation of (9), the matrices F and V, for the new infections and the remaining transfers are respectively, given by

$$F = B[F_1 + \text{diag}(S^0)F_2] \quad \text{and} \quad V = -V_y, \tag{22}$$

where $F_1 = [0, \text{diag}(\beta), 0, 0]$ and $F_2 = [0, 0, \text{diag}(\beta.\varepsilon), 0]$. Thus, the basic reproduction number is by

$$\mathcal{R}_0 = \rho(FV^{-1}) = \rho\left(B\left[F_1 + \text{diag}(S^0)\ F_2\right]\left(-V_y^{-1}\right)\right), \tag{23}$$

where ρ is the spectral radius of the matrix FV^{-1}.

The basic reproduction number $\mathcal{R}_0$, is the average number of secondary cases produced by a single infective individual which is introduced into an entirely susceptible population.

3.3 Global stability of the disease-free equilibrium

In this section, we address the global stability of the disease-free equilibrium of model system (7).

Theorem 2 *Consider model system (7) and assume that the mobility matrix* $\mathcal{M}$ *is irreducible. Then, the disease-free equilibrium* $P_0 = (S^0, 0, 0, 0, 0)$ *is globally asymptotically stable in* Ω *if* $\mathcal{R}_0 < 1$.

Proof The local stability of P_0 is classic by the result of van den Driessche and Watmough [40]. Since we are interested in the asymptotic behavior of the system (7), we will show that there exists $T > 0$ such that, if $\mathcal{R}_0 < 1$ then the solutions of (7) tend to the $P_0 = (S^0, 0, 0, 0, 0)$ when $t \to 0$, for $t > T$. Indeed, from the first equation of system (7), one has

$$\dot{S} \leq \pi - [\text{diag}(\mu) - \mathcal{M}]S. \tag{24}$$

This suggests the linear comparison system

$$\dot{X}_i = \pi - [\text{diag}(\mu) - \mathcal{M}]S. \tag{25}$$

The linear comparison system (25) has a unique positive equilibrium S^0 which is globally asymptotically stable. Since the matrix $[\text{diag}(\mu) - \mathcal{M}]$ is invertible and is a stable M-matrix [20], then, by the comparison theorem for cooperative systems, one has that

$$\limsup_{t\to\infty} S_i(t) \leq \lim_{t\to\infty} X_i(t) = S_i^0, \quad \text{for} \quad i = 1, \ldots, n. \tag{26}$$

Thus, for any $\sigma > 0$, there exists a sufficiently large $T > 0$ such that $S_i(t) \leq S_i^0 + \sigma$, for all $t > T$ and $i = 1, \ldots, n$.

Since $\mathcal{R}_0$ depend of S^0, we set $F = F(S^0)$, $S_\sigma^0 = S^0 + \sigma\mathbb{1}$ and $F_\sigma = F(S_\sigma^0) = F(S^0 + \sigma\mathbb{1}) = B[F_1 + \text{diag}(S^0 + \sigma\mathbb{1})F_2]$. Since the spectral radius of $F_\sigma V^{-1}$ is a continuous function of σ, we can choose σ as small as possible such that if $\rho(FV^{-1}) < 1$, then $\rho(F_\sigma V^{-1}) < 1$.

Now, since $S_i(t) \leq S_i^0 + \sigma$ for all $t > T$ and $\dfrac{S_i(t)}{N_i(t)} \leq 1$, then replacing $S_i(t)$ by $S_i^0 + \sigma$ in model system (7), we have the following comparison linear system in E, I, J and R:

$$\begin{cases} \dot{E} = \text{diag}(\mathbb{1} - p)[\text{diag}(\beta)I + \text{diag}(\varepsilon \cdot \beta)\text{diag}(S^0 + \sigma\mathbb{1})J] \\ \qquad + \text{diag}(\rho \cdot (\mathbb{1} - \theta))J - \text{diag}(A_E)E + \mathcal{M}E, \\ \dot{I} = \text{diag}(p \cdot f)[\text{diag}(\beta)I + \text{diag}(\varepsilon \cdot \beta)\text{diag}(S^0 + \sigma\mathbb{1})J] \\ \qquad + \text{diag}(\theta)J + \text{diag}(\gamma)R + \text{diag}(h \cdot (\mathbb{1} - \alpha) \cdot k)E \\ \qquad - \text{diag}(A_I)I + \eta\mathcal{M}I, \\ \dot{J} = \text{diag}(p \cdot (\mathbb{1} - f)[\text{diag}(\beta)I + \text{diag}(\varepsilon \cdot \beta) \\ \qquad \text{diag}(S^0 + \sigma\mathbb{1})J] + \text{diag}(\mathbb{1} - h) \cdot (\mathbb{1} - \alpha) \cdot k)E \\ \qquad - \text{diag}(A_J)J + \eta\mathcal{M}J, \\ \dot{R} = \text{diag}(r)I - \text{diag}(A_R)R + \mathcal{M}R, \end{cases} \tag{27}$$

System (27) can be written in the following compact form:

$$\dot{y} = (F_\sigma - V)\, y, \tag{28}$$

where y is defined as in Eq. (9). $y = (0, 0, 0, 0)$ is the unique equilibrium of this linear comparison system (28) which is globally asymptotically stable, since it is well known that if $s(F_\sigma - V)$ is the stability modulus of a matrix $(F_\sigma - V)$ defined as the maximal real part of the eigenvalues of $(F_\sigma - V)$, then from [40], $s(F_\sigma - V) < 0$ is equivalent to $\rho(F_\sigma V^{-1}) < 1$.

Therefore, all solutions of the linear comparison system (28) converge to the trivial solution $y = (0, 0, 0, 0)$ when t tend to $+\infty$, with $t > T$. It is obvious to see that since $\mathcal{M}$ is a Metzler matrice and is irreducible, then $F_\sigma - V$ as the jacobian of system (28) is a M-matrix and irreducible. Thus, by

comparison theorem for monotone dynamical systems [20], we can conclude that the E, I, J, R components of system (7) also converge to zero when $t \to \infty$, with $t > T$. Putting this last zero solution into the first equation of system (7) gives the linear system (25) which admits a unique positive equilibrium S^0 which is globally asymptotically stable. Finally, by the asymptotically autonomous systems theory [41], we can conclude that the S-component of the solution of system (7) converges to S^0. This proves the global attractiveness of $P_0 = (S^0, 0, 0, 0)$ when $\mathcal{R}_0 < 1$, and this completes the proof. □

3.4 Endemic equilibrium and bifurcation analysis for $\mathcal{R}_0$ near one

An endemic equilibrium is a stationary solution of system (7), with at least one positive infected state variable. It is very difficult to find an explicit formula of the endemic equilibrium point because model system (4) is complex. Alternatively, we give a simple criterion for the existence of an endemic equilibrium when $\mathcal{R}_0$ is near one. To do so, we shall proceed in the following two steps: i) study the model when the patches are isolated, and ii) analyze the bifurcation when theses patches are then connected by small migration flows. For all these cases, we shall use the implicit functions theorem result [42–44].

3.4.1 Case of isolated patches

We consider the case when the patches are isolated (i.e., there is no migration between them). In this case, $\mathcal{M} = 0$ and model system (4) becomes

$$\begin{cases} \dot{x}_i = \varphi_i(x_i) - \lambda_i x_i, \\ \dot{y}_i = \lambda B_i x + A_i\, y_i, \end{cases} \tag{29}$$

where $x_i = S_i \in \mathbb{R}_+$ is a state representing the compartment of non transmitting individuals (susceptible), $y_i = (E_i, I_i, J_i, R_i)^T \in \mathbb{R}_+^4$ is the vector representing the state compartment of different infected individuals (latently infected, diagnosed and undiagnosed infectious and recovered individuals), $\varphi_i(x_i) = \pi_i - \mu_i\, x_i$, $\lambda_i = \dfrac{\langle e_{i_1} \mid y_i \rangle}{N_i} + \langle e_{i_2} \mid y_i \rangle$ is the force of infection, $e_{i_1} = (0, \beta_i, 0, 0)$, $e_{i_2} = (0, 0, \beta_i \varepsilon_i, 0)$, $B_i = (1 - p_i, p_i f_i, p_i(1 - f_i), 0)^T$, $\langle . \mid . \rangle$ is the usual scalar product and A_i is the constant matrix:

$$A_i = \begin{bmatrix} -A_{E_i} & 0 & \delta_i(1-\theta_i) & 0 \\ k_i h_i (1-\alpha_i) & -A_{I_i} & \theta_i & \gamma_i \\ k_i(1-h_i)(1-\alpha_i) & 0 & -A_{J_i} & 0 \\ 0 & r_i & 0 & -A_{R_i} \end{bmatrix},$$

with A_{E_i}, A_{I_i}, A_{J_i} and A_{R_i} defined as in Eq. (4). Note that A_i is a Metzler matrix with negative column sums, thus non-singular. Since A_i is a non-singular Metzler matrix (similar proof to Theorem 1), $-A_i^{-1}$ is nonnegative [38,39]. We will need this property later. It can be shown that V_y is a block diagonal matrix, where each block is defined by A_i. The matrix F for the new infection terms is

$$F_i = B_i \left(e_{i1} + e_{i2} S_i^0 \right) = \begin{pmatrix} 0 & \beta_i(1-p_i) & \beta_i \varepsilon_i (1-p_i) S_i^0 & 0 \\ 0 & \beta_i p_i f_i & \beta_i \varepsilon_i p_i f_i S_i^0 & 0 \\ 0 & \beta_i p_i (1-f_i) & \beta_i \varepsilon_i p_i (1-f_i) S_i^0 & 0 \\ 0 & 0 & 0 & 0 \end{pmatrix},$$

where $S_i^0 = \dfrac{\pi_i}{\mu_i}$.

Let $\mathcal{R}_0^{(i)}$ be the basic reproduction number of the isolated patch i. Using the method of van den Driessche and Watmough [40], the basic reproduction number $\mathcal{R}_0(0)$ of the metapopulation model (4) when the patches are isolated (i.e., $m_{ij} = m_{ji} = 0$ for all i, j) is given by

$$\mathcal{R}_0 = \mathcal{R}_0(0) = \max_{i=1,\ldots,n} \mathcal{R}_0^{(i)}, \tag{30}$$

where

$$\mathcal{R}_0^{(i)} = R_{01}^i + \frac{\pi_i}{\mu_i} R_{02}^i,$$

with

$$\mathcal{R}_{01}^i = \left\langle e_{i_1} \mid \left(-A_i^{-1} \right) B_i \right\rangle \quad \text{and} \quad \mathcal{R}_{02}^i = \left\langle e_{i_2} \mid \left(-A_i^{-1} \right) B_i \right\rangle.$$

Now, let us compute the endemic equilibrium. Let $Q_i^\star = (x_i^\star, y_i^\star)$ be any arbitrary equilibrium of model system (29) (i.e., a steady state with $y_i^\star \neq 0$), then for any i, $x_i^\star$ and $y_i^\star$) are solutions of the following system:

$$\begin{cases} \varphi_i(x_i^\star) - \lambda_i^\star x_i^\star = 0, \\ \lambda_i^\star x_i^\star B_i + A_i\, y_i^\star = 0, \end{cases} \tag{31}$$

where $\varphi_i(x_i^\star) = \pi_i - \mu_i x_i^\star$ and

$$\lambda_i^\star = \frac{\langle e_{i_1} \mid y_i^\star \rangle}{N_i^\star} + \langle e_{i_2} \mid y_i^\star \rangle, \tag{32}$$

is the force of infection evaluated at the steady state. Multiply the second equation of Eq. (31) by $-A_i^{-1}$ yields

$$y_i^\star = \lambda_i^\star x_i^\star \left(-A_i^{-1} \right) B_i. \tag{33}$$

With this in mind, one can deduce that

$$\langle e_{i_1} \mid y_i^\star \rangle = \lambda_i^\star x_i^\star \mathcal{R}_{01}^i \quad \text{and} \quad \langle e_{i_2} \mid y_i^\star \rangle = \lambda_i^\star x_i^\star \mathcal{R}_{02}^i. \tag{34}$$

From the first equation of Eq. (31), one has

$$x_i^\star = \frac{\pi_i}{\mu_i + \lambda_i^\star}. \tag{35}$$

Combining Eqs. (32), (34) and (35) yields the total population of patch i at the steady state:

$$N_i^\star = \frac{\lambda_i^\star \pi_i \mathcal{R}_{01}^i}{\lambda_i^\star(\lambda_i^\star + \mu_i - \pi_i \mathcal{R}_{02}^i)}. \tag{36}$$

Now, let $w_1^i = (1,0,0,0)^T$, $w_2^i = (0,1,0,0)^T$, $w_3^i = (0,0,1,0)^T$ and $w_4^i = (0,0,0,1)^T$. Then, from Eq. (33), we have

$$\begin{aligned}
E_i^\star &= \langle w_1^i \mid y_i^\star \rangle = \lambda_i^\star x_i^\star \langle w_1^i \mid (-A_i^{-1})B_i \rangle = \lambda_i^\star x_i^\star a_{E_i},\\
I_i^\star &= \langle w_1^i \mid y_i^\star \rangle = \lambda_i^\star x_i^\star \langle w_2^i \mid (-A_i^{-1})B_i \rangle = \lambda_i^\star x_i^\star a_{I_i},\\
J_i^\star &= \langle w_3^i \mid y_i^\star \rangle = \lambda_i^\star x_i^\star \langle w_3^i \mid (-A_i^{-1})B_i \rangle = \lambda_i^\star x_i^\star a_{J_i},\\
R_i^\star &= \langle w_4^i \mid y_i^\star \rangle = \lambda_i^\star x_i^\star \langle w_4^i \mid (-A_i^{-1})B_i \rangle = \lambda_i^\star x_i^\star a_{R_i},
\end{aligned} \tag{37}$$

where

$$a_{E_i} = \langle w_1^i \mid (-A_i^{-1})B_i \rangle, \quad a_{I_i} = \langle w_2^i \mid (-A_i^{-1})B_i \rangle,$$

$$a_{J_i} = \langle w_3^i \mid (-A_i^{-1})B_i \rangle \quad \text{and} \quad a_{R_i} = \langle w_4^i \mid (-A_i^{-1})B_i \rangle.$$

Now, using Eq. (5) in the absence of migration at the steady state and Eq. (37), one has

$$N_i^\star = \frac{\pi_i}{\mu_i} \frac{\mu_i + \lambda_i^\star(1 - d_i a_{I_i} - \delta_i a_{J_i})}{\lambda_i^\star + \mu_i}. \tag{38}$$

Equaling Eqs. (36) and (38), it can be shown that the nonzero endemic equilibria of model system (9) satisfies the following quadratic equation in term of $\lambda_i^\star$:

$$c_2(\lambda_i^\star)^2 + c_1(\lambda_i^\star) + c_0 = 0, \tag{39}$$

where

$$c_2 = \mu_i(a_{E_i} + a_{I_i} + a_{J_i} + a_{R_i}),$$

$$c_1 = (d_i a_{I_i} + \delta_i a_{J_i})(\pi_i R_{02}^i - \mu_i) + \mu_i(1 - \mathcal{R}_0^{(i)}),$$

$$c_0 = \mu_i^2(1 - \mathcal{R}_0^{(i)}).$$

The positive endemic equilibria $Q_i^\star$ are obtained by solving the polynomial equation $c_2(\lambda_i^\star)^2 + c_1(\lambda_i^\star) + c_0 = 0$ with respect to $\lambda_i^\star$ and substituting the result (positive values of $\lambda_i^\star$) into the expressions of the state variables at the steady state. It is worth noting that the coefficient c_2 is positive, while the coefficient c_0 is positive when $\mathcal{R}_0^i < 1$ and negative when $\mathcal{R}_0^i > 1$. Thus, the number of possible real roots of the polynomial equation (39) depends on the signs of c_1 and c_0. This can be analyzed using the Descartes Rule of Signs on the polynomial equation $f(\lambda_i^\star) = c_2(\lambda_i^\star)^2 + c_1(\lambda_i^\star) + c_0$. Observe that, if $\mathcal{R}_0^i > 1$, then $c_0 < 0$ and Eq. (39) has exactly one positive solution. Solving the quadratic equation (39), the positive solution is given by

$$\lambda_i^\star = \frac{-c_1 + \sqrt{c_1^2 - 4c_0c_2}}{2c_2}, \tag{40}$$

Hence, we have proved the following result.

Theorem 3 *Assume that all the patches are disconnected (there is no migration between them). Then, for each patch i, if $\mathcal{R}_0^{(i)} > 1$, then model system (4) has a unique endemic equilibrium $Q^\star = (Q_i^\star)_{i=1,\ldots,n}$, with $Q_i^\star = (S_i^\star, E_i^\star, I_i^\star, J_i^\star, R_i^\star)$ where $S_i^\star$, $E_i^\star$, $I_i^\star$, $J_i^\star$ and $R_i^\star$ are defined as in Eqs. (35), (37)–(40).*

3.4.2 Equilibria with small migrations rates between patches: bifurcation analysis near $\mathcal{R}_0 = 1$

Herein, we shall prove that, if the metapopulation is at an endemic steady state in the absence of migration, it will remains so as long as the patches are connected with small migration rates so that the overall basic reproduction number (depending yet on the migration rates) is greater than the unity.

To address this issue, let us written system (7) in the following form:

$$F(M, X) = 0, \tag{41}$$

where $X = (S_1, E_1, I_1, J_1, R_1, \ldots, S_n, E_n, I_n, J_n, R_n) \in \mathbb{R}_+^{5n}$, $M = (m_{12}, \ldots, m_{1n}, \ldots, m_{n1}, \ldots, m_{n-1\,n}) \in \mathbb{R}^{n(n-1)}$ is the vector of migration and $F = (f_1, \ldots, f_{5n})$.

Now, let

$$\begin{aligned}
\mathcal{R}_0 : \mathbb{R}^{n(n-1)} &\longrightarrow \mathbb{R}\\
M &\longrightarrow \mathcal{R}_0(M).
\end{aligned}$$

be the basic reproduction number depending on the migration vector M. We have the following result.

Lemma 4 *When $\mathcal{R}_0(0) > 1$, there exists a neighborhood $U_1 \subset \mathbb{R}^{n(n-1)}$ of $M = 0$ such that $\mathcal{R}_0(M) > 1, \quad \forall M \in U_1$.*

This result is a consequence of the continuity property of eigenvalues of a matrix with respect to each of its entries [45]. Now, using Lemma 4, we claim the following result:

Lemma 5 *The following two conditions are satisfied.*

1. *There exists a neighborhood U_2 of 0 and a neighborhood $\mathcal{V}$ of $Q^\star$ such that f_i is $\mathcal{C}^1$ in a neighborhood $U_2 \times \mathcal{V} \subset \mathbb{R}^{n(n-1)} \times \overset{\circ}{\Omega}$ of $(0, Q^\star)$ where $\overset{\circ}{\Omega}$ is the interior of Ω.*
2. $\left(\dfrac{\partial f_i}{\partial x_j}(0, Q^\star)\right)_{i,j=1}^{5n}$ *is a non-singular matrix.*

Proof The proof of this result follows from the properties of the matrices therein. Indeed, f_i is a $\mathcal{C}^1$ function on any neighborhood $U_2 \times \mathcal{V} \subset \mathbb{R}^{n(n-1)} \times \overset{\circ}{\Omega}$ of $(0, Q^\star)$ since f_i is a linear combination of $\mathcal{C}^1$ functions. On the other hand, $\left(\dfrac{\partial f_i}{\partial x_j}(0, Q^\star)\right)_{i,j=1}^{5n} = \operatorname{diag}(W_i)$ is a diagonal block matrix where each diagonal block is defined by

$$W_i = \begin{pmatrix} -\beta_i A_i^* - \mu_i & \beta_i B_i^* & -\beta_i C_i^* & \beta_i D_i^* & \beta_i F_i^* \\ (1-p_i)\beta_i A_i^* & -G_{i1} & (1-p_i)\beta_i C_i^* & G_{i2} & (1-p_i)\beta_i F_i^* \\ p_i f_i \beta_i A_i^* & G_{i3} & p_i f_i \beta_i C_i^* - A_{I_i} & p_i f_i \beta_i D_i^* + \theta_i & p_i f_i \beta_i F_i^* + \gamma_i \\ p_i(1-f_i)\beta_i A_i^* & G_{i4} & p_i(1-f_i)\beta_i C_i^* & G_{i5} & p_i(1-f_i)\beta_i F_i^* \\ 0 & 0 & r_i & 0 & -A_{R_i} \end{pmatrix}$$

where

$$A_i^* = \frac{I_i^\star(N_i^\star - S_i^\star)}{(N_i^\star)^2} + \varepsilon_i J_i^\star, \qquad B_i^* = \frac{I_i^\star S_i^\star}{(N_i^\star)^2},$$
$$C_i^* = \frac{S_i^\star(N_i^\star - I_i^\star)}{(N_i^\star)^2}, \qquad D_i^* = \frac{I_i^\star S_i^\star}{(N_i^\star)^2} - \varepsilon_i,$$
$$F_i^* = \frac{I_i^\star S_i^\star}{(N_i^\star)^2}, \qquad G_{i1} = -(1-p_i)\beta_i B_i^* + A_{E_i},$$
$$G_{i2} = (1-p_i)\beta_i D_i^* + \rho_i(1-\theta_i),$$
$$G_{i3} = -p_i f_i \beta_i B_i^* + h_i k_i (1-\alpha_i),$$
$$G_{i4} = -p_i(1-f_i)\beta_i B_i^* + k_i(1-h_i)(1-\alpha_i) \quad \text{and}$$
$$G_{i5} = p_i(1-f_i)\beta_i D_i^* - A_{J_i}.$$

It then follows that $\left(\dfrac{\partial f_i}{\partial x_j}(0, Q^\star)\right)_{i,j=1}^{5n}$ is invertible if and only if W_i, $i = 1, \ldots, n$ are invertible. Since W_i are strictly diagonal column dominant matrices, then, they are non-singular (similar proof to Theorem 1). It follows that the determinant of $\left(\dfrac{\partial f_i}{\partial x_j}(0, Q^\star)\right)_{i,j=1}^{5n}$ is non-zero. This achieves the proof. □

Now, applying the implicit function theorem [42], the following result is straightforward:

Theorem 4 *The equation $F(M, X) = 0$ has a unique solution $\overline{Q} \in \mathcal{V}$ defined by $\overline{Q} = \varphi(M)$ where $\varphi : \mathcal{V} \to U = U_1 \cap U_2$ is a function such* $\lim_{X \to \overline{Q}} \varphi(X) = Q^\star$.

Remark 2 It is worth noting that Theorem 4 holds for small migrations rates (i.e., $M \in U_1$). We do not pretend to have the same result in the case of high rates of migrations (i.e., those migrations rates which are not in a neighborhood U_1). In addition, a similar theorem as Theorem 4 can be proved when $\mathcal{R}_0 < 1$.

The above theorem says that, if the isolated metapopulation is disease free, then a suitable choice of (small) migration rates would not change the metapopulation disease status, maintaining it free of disease. To summarize, if we use directly the quantity $\mathcal{R}_0$ to control the TB in patchy environment, we must lower $\mathcal{R}_0$ below one to prevent it.

4 Numerical simulations

In order to illustrate the results of the foregoing analysis, numerical simulations of system (4) was carried out on three and fifteen patches. The parameter values used for numerical simulations are given in Table 1. In all simulations, the standard method of Runge Kutta of fourth order with adaptive stepsize was used in Matlab R2010b.

4.1 A three-patches model

4.1.1 Population dynamics in the absence of migration

In the absence of migration, ($m_{ij} = m_{ji} = 0$), lets choose $\beta_1 = 1.5$, $\beta_2 = 0.8$ and $\beta_3 = 0.3$ (so that $\mathcal{R}_0^{(1)} = 1.3620 > 1$, $\mathcal{R}_0^{(2)} = 0.7064 < 1$ and $\mathcal{R}_0^{(3)} = 0.3126 < 1$) and keep all other parameter values as in Table 1. It appears as expected that TB dies out in other patches, but persist in patches where $\mathcal{R}_0 < 1$ (patch 2 and 3) and persist in the patch 1 (Fig. 3).

4.1.2 Impact of migration between patches on $\mathcal{R}_0$

All parameter values are summarized in Table 1.

• All patches are not connected two by two

Considering the hypothetical scenario of TB spread between a high prevalence endemic region (patch 1) and low prevalence regions where the outbreak could be eradicated (patches 2 and 3), let $\beta_1 = 1.5$, $\beta_2 = 0.8$, $\beta_3 = 0.3$ and $\eta = 0.5$ (so that $\mathcal{R}_0^{(1)} = 1.3620 > 1$, $\mathcal{R}_0^{(2)} = 0.7064 < 1$ and $\mathcal{R}_0^{(3)} = 0.3126 < 1$) in the absence of migration between patches 2 and 3 ($m_{23} = m_{32} = 0$). This corresponds to the case when to travel from patch 3 to patch 2 and from patch 2 to patch 3, one must pass in patch 1. People in the patch with lower disease transmission rate are oblige to pass in the

Table 1 Numerical values for the parameters of model system (4) in patch i

Symbol	Value	Source	Symbol	Value	Source
π_i	1000, 900, 1200/year	Assumed	β_i	Variable	Assumed
p_i	0.11	[46]	f_i	0.74	[24]
ε_i	0.0003	Assumed	k_i	0.0003/year	Assumed
μ_i	1/53.4/year	[47]	d_i	0.139/year	[26]
α_i	0.001/year	[48]	h_i	0.74/year	[48]
r_i	0.7372/year	[48]	ρ_i	0.139 /year	[24]
γ_i	0.0986/year	[48]	θ_i	0.74/year	[48]
η	Variable	Assumed	δ_i	0.25/year	[26]
m_{ij}	Variable	Assumed	m_{ji}	Variable	Assumed

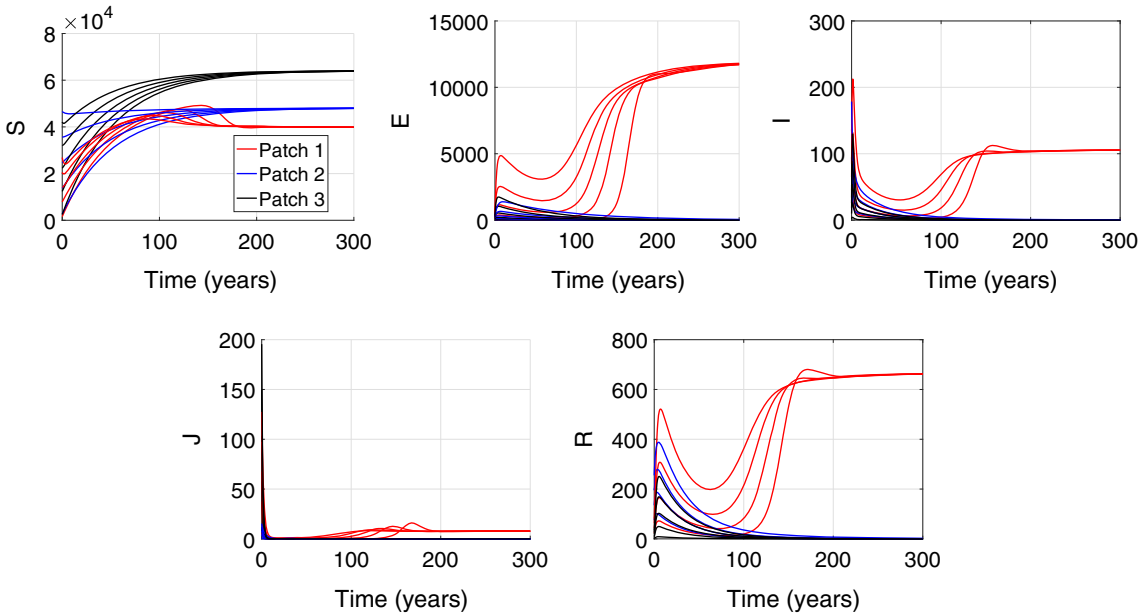

Fig. 3 Simulation results of model system (4) using various initial conditions when $m_{ij} = 0$ with $i, j = 1, 2, 3$, $\beta_1 = 1.5$, $\beta_2 = 0.8$ and $\beta_3 = 0.3$ (so that $\mathcal{R}_0^{(1)} = 1.3620 > 1$, $\mathcal{R}_0^{(2)} = 0.7064 < 1$ and $\mathcal{R}_0^{(3)} = 0.3126 < 1$). (S) Susceptible individuals, (E) latently infected individuals; (I) diagnosed infectious individuals, (J) undiagnosed infectious and (R) recovered individuals. Populations in patches 1, 2 and 3 are depicted in *red*, *blue* and *black lines*, respectively. All other parameter values are as in Table 1. (Color figure online)

patch where TB is endemic to go to another patch with lower disease transmission.

For $m_{12} = 0.05$ and $m_{13} = 0.05$, an increase of the travel rate from patch 1 (the patch with higher disease transmission rate) to patches 2 and 3 (the patches with lower disease transmission rate) may result to a decrease of $\mathcal{R}_0$ (Fig. 4a, b). Moreover, for large values of the migration rates ($m_{21} > 0.05$ and $m_{31} > 0.09$), the disease could died out since $\mathcal{R}_0 < 1$. The migration to patches with lower transmission might lead to a better control of the disease spread between patches. However, an increase of the migration rate to the patch with higher transmission rate might lead to an increase of $\mathcal{R}_0$ (Fig. 4c, d).

If Tb is endemic in patches 2 and 3, but not in patch 1 (Chosing $\beta_1 = 0.5$, $\beta_2 = 1.30$ and $\beta_3 = 1.2$, so that $\mathcal{R}_0^{(1)} = 0.5160$, $\mathcal{R}_0^{(2)} = 1.1478$, and $\mathcal{R}_0^{(3)} = 1.2505$), for $m_{23} = m_{32} = 0$, $m_{12} = 0.05$, $m_{13} = 0.05$ and $\eta = 0.5$, an increase in the migration rate from the patch with lower disease transmission rate to the patches where TB is endemics might lead to a generalized epidemic in all patches (Fig. 5a, b). An increase of the emigration rate from TB endemic patches will also lead to an increase of the $\mathcal{R}_0$.

• All patches are connected

Considering a patch with high prevalence (patch 1) and low prevalence regions where strategies was set down to control TB outbreak (patches 2 and 3), values of $\beta_1 = 1.5$, $\beta_2 = 0.8$ and $\beta_3 = 0.3$ (so that $\mathcal{R}_0^{(1)} = 1.3620 > 1$, $\mathcal{R}_0^{(2)} = 0.7064 < 1$ and $\mathcal{R}_0^{(3)} = 0.3126 < 1$), $\eta = 0.5$, $m_{23} = m_{32} = 0.05$ and $m_{12} = m_{13} = 0.04$ was chosen. It came out that with the chosen parameters, increasing the emigration rate from the endemic patch might lead to the control of the disease

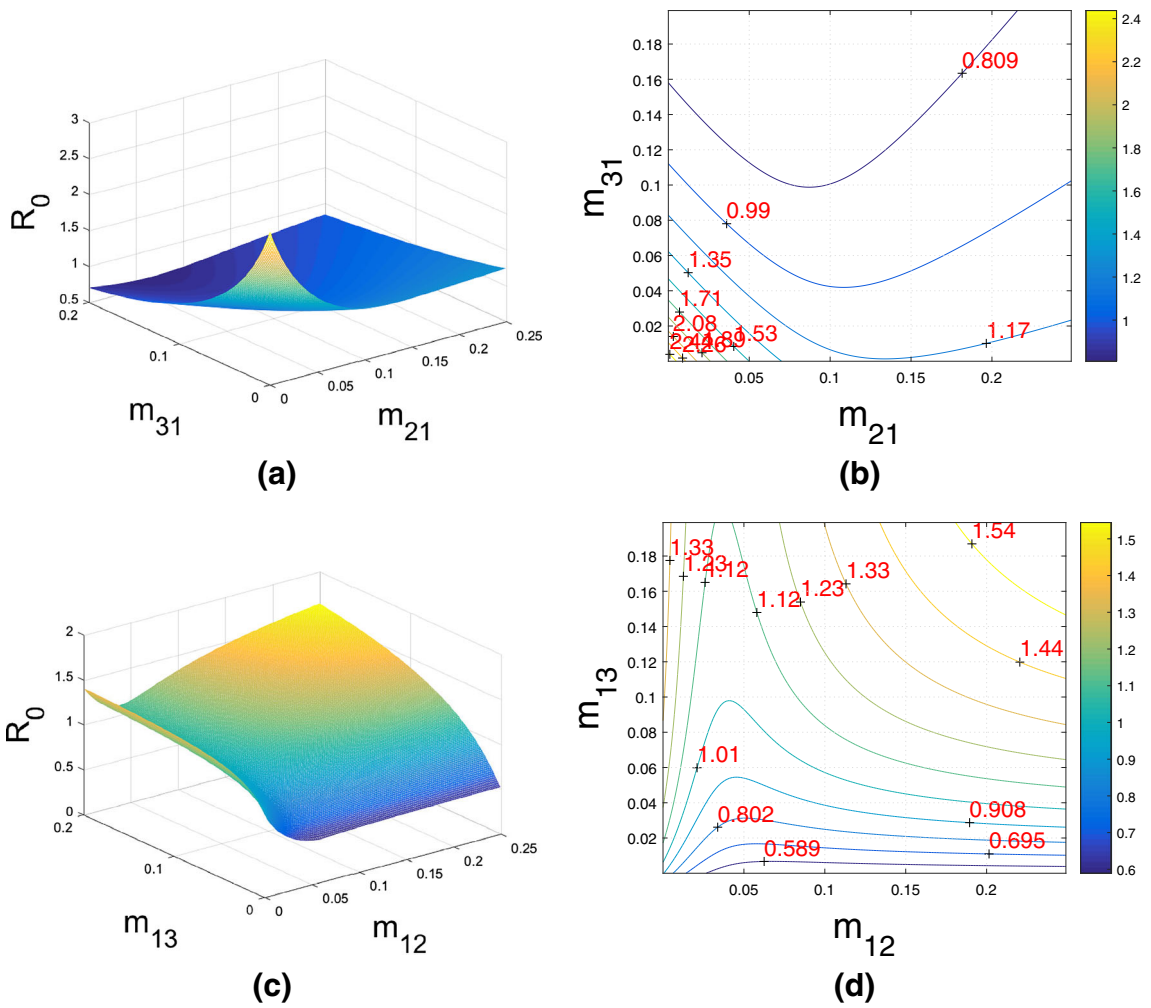

Fig. 4 **a**, **c** 3D and **b**, **d** contour plot showing the effects of the migration rates to and from the patch with higher transmission m_{21} and m_{31} on the basic reproduction number $\mathcal{R}_0$ when $\beta_1 = 1.5$, $\beta_2 = 0.8$, $\beta_3 = 0.3$, $\eta = 0.5$ and $m_{23} = m_{32} = 0$ (so that $\mathcal{R}_0^{(1)} = 1.3620 > 1$, $\mathcal{R}_0^{(2)} = 0.7064 < 1$ and $\mathcal{R}_0^{(3)} = 0.3126 < 1$). **a**, **b** $m_{12} = 0.05$ and $m_{13} = 0.05$; **c**, **d** $m_{21} = 0.04$ and $m_{31} = 0.04$. All other parameter values are as in Table 1

(Fig. 6a, b) while increasing the migration rate to endemic patch might lead to a global epidemic (Fig. 6c, d).

It was observed that including the migration between patch 2 and 3 did not change the result of the previous subsection.

4.1.3 Travel restriction of infectious

Let η be in the set $(0; 1)$, varying from the situation where the public health authorities can restrict completely or not the migration of active TB cases between all patches. Let $\beta_1 = 1.5$, $\beta_2 = 0.8$ and $\beta_3 = 0.3$ (so that $\mathcal{R}_0^{(1)} = 1.3620$, $\mathcal{R}_0^{(2)} = 0.7064$ and $\mathcal{R}_0^{(3)} = 0.3126$). Assuming the same migration rate between all patches, it comes out that the migration restriction might lead to the persistence of the disease $m_{32} = m_{23} = m_{13} = m_{31} = m_{12} = m_{21} = m = 0.2$ in the endemic patch (Fig. 7)

4.2 A fifteen-patches model

The interaction between a metapopulation network consisting of fifteen patches (Fig. 8) was analysed to access the disease propagation between patches. This configuration is realistic in many regions of sub-Saharan Africa when to go in a village, one must pass through several villages before arriving.

Following possibilities was considered: when the class with higher disease outbreak is at the center of the patches chain (patch 8) and the patch where it is in a corner. We assumed $m_{i\,i+1} = m_{i-1\,i} = m$, $i = 2, \ldots, 14$, $m_{1\,2} = m_{15\,14} = m$, and $m_{ij} = 0$ for $j \neq i - 1$ and $j \neq i + 1$ and when the outbreak starts from patch 1. Let set $\beta_i \in (0.2, 0.71)$ and $\pi_i \in (500; 1900)$ (so that $\mathcal{R}_0^{(1)} = 1.6589$, $\mathcal{R}_0^{(2)} = 0.6037$, $\mathcal{R}_0^{(3)} = 0.4673$, $\mathcal{R}_0^{(4)} = 0.9251$, $\mathcal{R}_0^{(5)} = 0.7725$, $\mathcal{R}_0^{(6)} = 0.7496$, $\mathcal{R}_0^{(7)} = 0.5587$, $\mathcal{R}_0^{(8)} = 0.6753$,

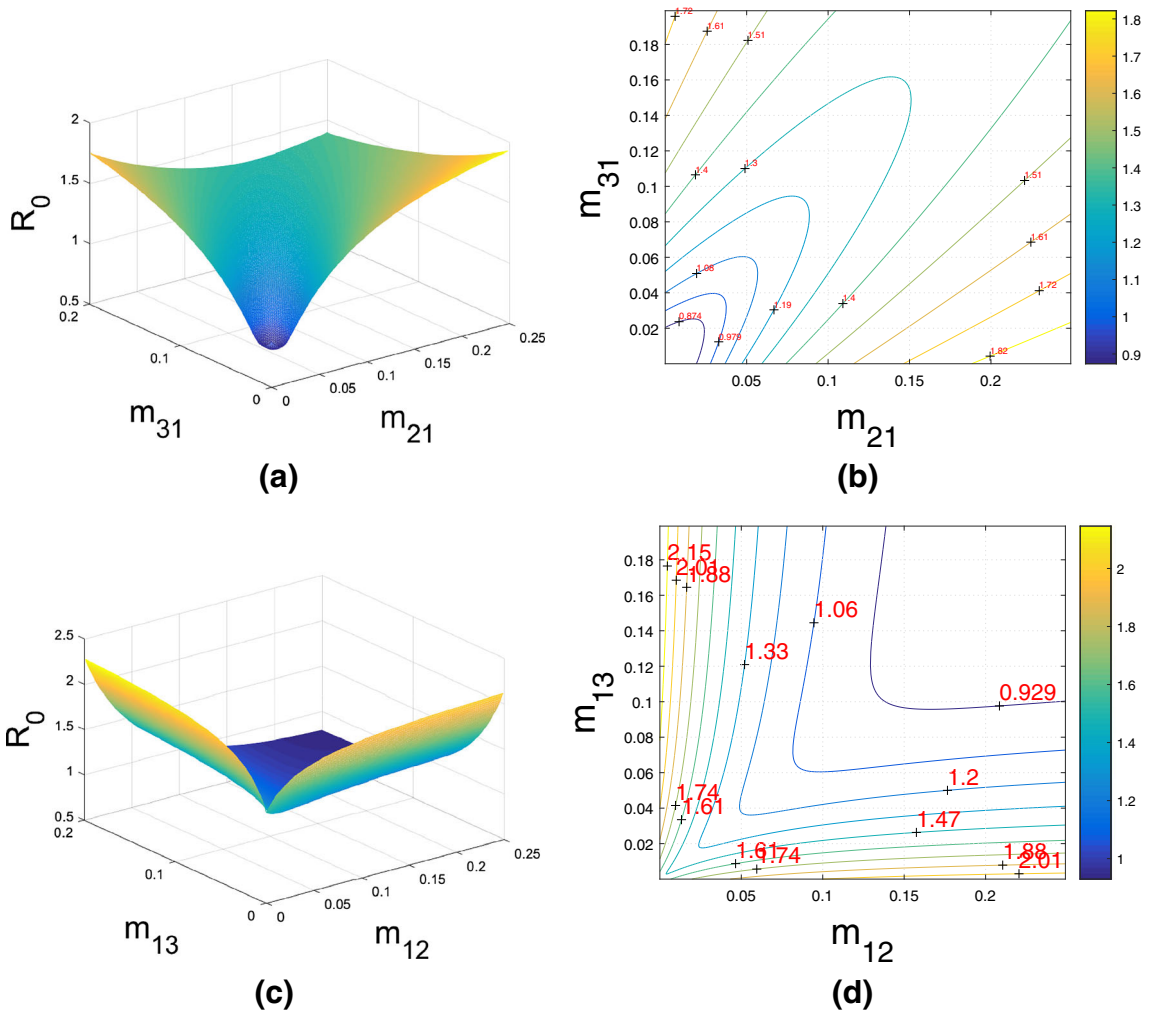

Fig. 5 **a**, **c** 3D and **b**, **d** contour plot showing the effects of the migration rates to and from the patch with higher transmission m_{21} and m_{31} on the basic reproduction number $\mathcal{R}_0$ when $\beta_1 = 0.5$, $\beta_2 = 1.30$, $\beta_3 = 1.2$, $\eta = 0.5$, $m_{23} = m_{32} = 0$, (so that $\mathcal{R}_0^{(1)} = 0.5160$, $\mathcal{R}_0^{(2)} = 1.1478$ and $\mathcal{R}_0^{(3)} = 1.2505$). **a**, **b** $m_{12} = 0.05$ and $m_{13} = 0.05$; **c**, **d** $m_{21} = 0.04$ and $m_{31} = 0.04$. All other parameter values are as in Table 1

$\mathcal{R}_0^{(9)} = 0.8468$, $\mathcal{R}_0^{(10)} = 0.4731$, $\mathcal{R}_0^{(11)} = 0.6268$, $\mathcal{R}_0^{(12)} = 0.1563$, $\mathcal{R}_0^{(13)} = 0.2728$, $\mathcal{R}_0^{(14)} = 0.7266$, and $\mathcal{R}_0^{(15)} = 0.8750$). This is the case where to travel from the first patch to the last, one needs to go through all other patches.

The initial size of the total population in all patches is given by

$$N(0) = (9052, 8110, 9120, 8532, 10034, 9028, 8035, 14042, 8828, 1356, 2231, 10627, 12550, 1456, 2675).$$

These initial conditions was chosen arbitrarily. Firstly, we considered that the disease is endemic in patch 1 and we study the propagation of TB in other patches.

Figure 9 presents the prevalence of the disease when $m = 0.04$ in all patches. From this figure, it is evident that when TB is endemic in patch 1 ($\mathcal{R}_0^{(1)} = 1.6046$), people in patch 2 will be infected, and nearby patches also. The disease propagation will not be effective after the fourth patch.

Let us consider the case when TB is endemic inside the patch 8 and not endemic elsewhere by setting $\eta = 1$, $\beta_i \in (0.2, 0.71)$ and $\pi_i \in (500; 1900)$ (so that $\mathcal{R}_0^{(1)} = 0.7137$, $\mathcal{R}_0^{(2)} = 0.6037$, $\mathcal{R}_0^{(3)} = 0.4673$, $\mathcal{R}_0^{(4)} = 0.9251$, $\mathcal{R}_0^{(5)} = 0.7725$, $\mathcal{R}_0^{(6)} = 0.7496$, $\mathcal{R}_0^{(7)} = 0.5587$, $\mathcal{R}_0^{(8)} = 1.4878$, $\mathcal{R}_0^{(9)} = 0.8468$, $\mathcal{R}_0^{(10)} = 0.4731$, $\mathcal{R}_0^{(11)} = 0.6268$, $\mathcal{R}_0^{(12)} = 0.1563$, $\mathcal{R}_0^{(13)} = 0.2728$, $\mathcal{R}_0^{(14)} = 0.7266$, and $\mathcal{R}_0^{(15)} = 0.8750$) and other parameter values as in Fig. 9.

The prevalence of the disease in the community, defined as the ratio of infectious by the total population, when $m = 0.04$ is presented in Fig. 10. This figure illustrates that when TB is endemic in patch 8 ($\mathcal{R}_0^{(8)} = 2.6943$), the disease will begin to infect all their neighbors patches. Thus, the impact of the disease is more important than in Fig. 9, when the patch was at the corner. One can also see that the number of cases in other paches growth with the number of infectious in patch 8 and the size of the population of the patch 8.

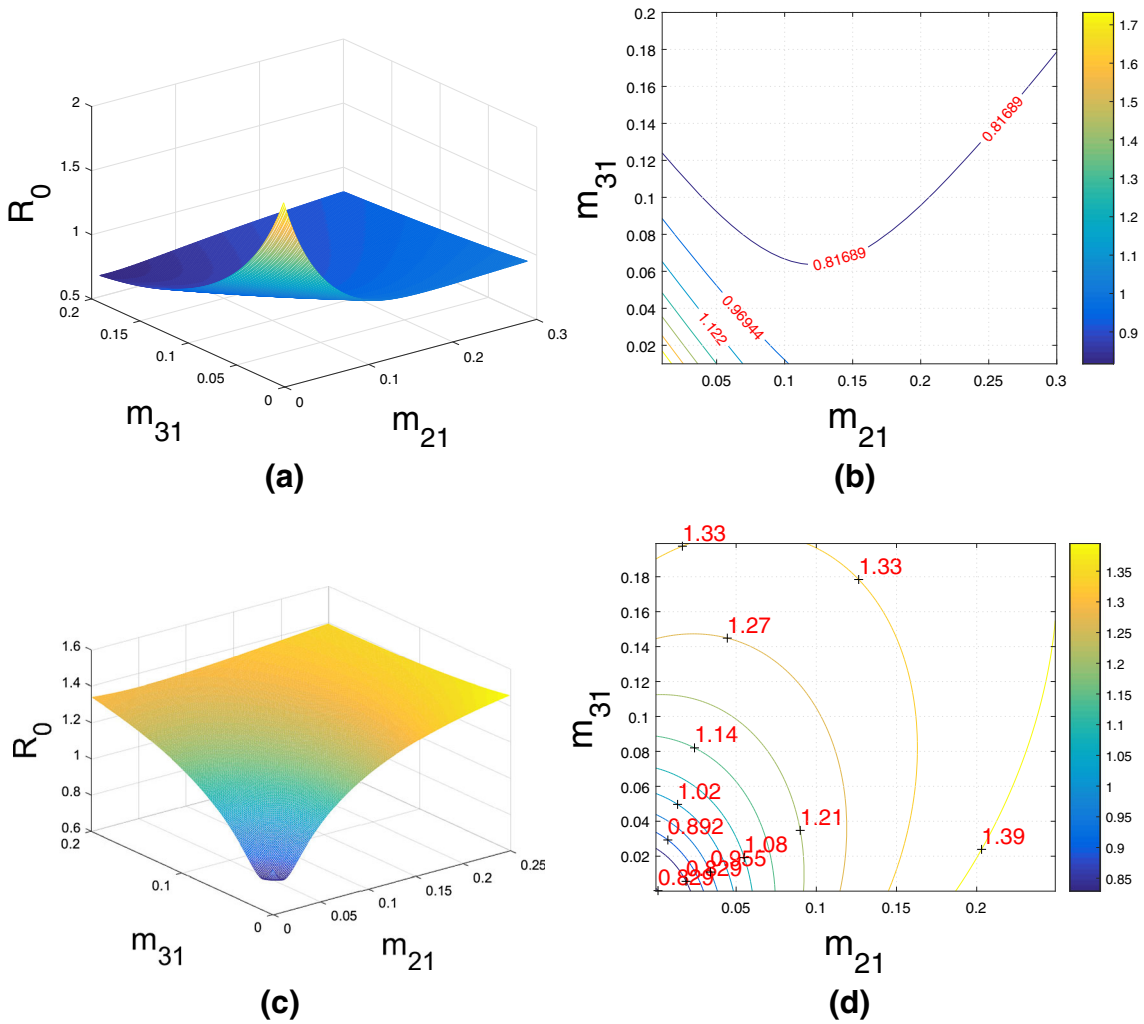

Fig. 6 **a**, **c** 3D and **b**, **d** contour plot showing the effects of the migration rates to and from the patch with higher transmission m_{21} and m_{31} on the basic reproduction number $\mathcal{R}_0$ when $\beta_1 = 0.5$, $\beta_2 = 1.30$, $\beta_3 = 1.2$, $\eta = 0.5$, $m_{23} = m_{32} = 0.05$ (so that $\mathcal{R}_0^{(1)} = 0.5160$, $\mathcal{R}_0^{(2)} = 1.1478$ and $\mathcal{R}_0^{(3)} = 1.2505$). **a**, **b** $m_{12} = 0.05$ and $m_{13} = 0.05$; **c**, **d** $m_{21} = 0.04$ and $m_{31} = 0.04$. All other parameter values are as in Table 1

4.2.1 General dynamics with travel restriction

Let us assumed that the initial size of the total population in the patch with higher endemicity vary, while the initial population size in other patches is constant. These initial conditions was chosen arbitrarily. Firstly, we consider that the disease is endemic in patch 1 and we study the propagation in other patches.

Figure 11 presents the prevalence of the disease when $m = 0.05$ in each patch. From, this figure it is evident that when TB is endemic in patch 1 ($\mathcal{R}_0^{(1)} = 1.6046$), the disease will spread into the closest neighbor patches. Comparing to the case of Fig. 9, one can see that, the propagation of the disease is slow than before and the number of infectious is less important. But the spread of the disease will be effective despite the slow progression.

Now, let us consider the case when TB is endemic inside the patch 8 and not endemic elsewhere. We set $\eta = 1$ and $\beta_i \in (0.2, 0.71)$, $\pi_i \in (500; 1900)$ (so that $\mathcal{R}_0^{(1)} = 0.7137$, $\mathcal{R}_0^{(2)} = 0.6037$, $\mathcal{R}_0^{(3)} = 0.4673$, $\mathcal{R}_0^{(4)} = 0.9251$, $\mathcal{R}_0^{(5)} = 0.7725$, $\mathcal{R}_0^{(6)} = 0.7496$, $\mathcal{R}_0^{(7)} = 0.5587$, $\mathcal{R}_0^{(8)} = 1.4878$, $\mathcal{R}_0^{(9)} = 0.8468$, $\mathcal{R}_0^{(10)} = 0.4731$, $\mathcal{R}_0^{(11)} = 0.6268$, $\mathcal{R}_0^{(12)} = 0.1563$, $\mathcal{R}_0^{(13)} = 0.2728$, $\mathcal{R}_0^{(14)} = 0.7266$, and $\mathcal{R}_0^{(15)} = 0.8750$). All other parameter values are defined as in Fig. 9.

The prevalence of the disease in the community and the number of infective population when $m = 0.04$ is presented in Fig. 12. The initial conditions have been chosen as in Fig. 9. This figure illustrates that when TB is endemic in patch 8 ($\mathcal{R}_0^{(8)} = 2.6943$), the disease will begin to infect all their neighbors patches. This illustrates that the effect of the migration will be less in neighbors patches than in Fig. 10.

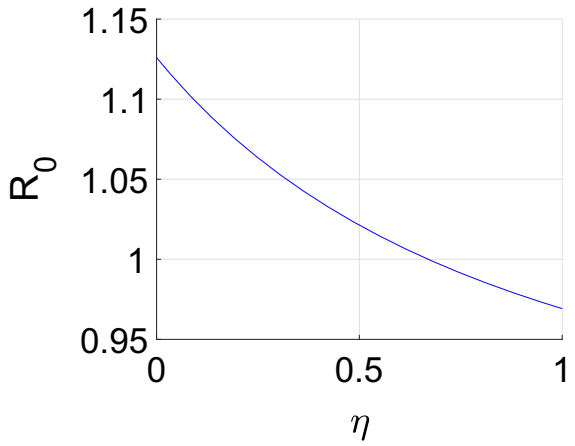

Fig. 7 Variation of the basic reproduction ratio as ($\mathcal{R}_0$) a function of capacity of active infected population to move between patches for $\beta_1 = 1.5$, $\beta_2 = 0.8$ and $\beta_3 = 0.3$ (so that $\mathcal{R}_0^{(1)} = 1.3620 > 1$, $\mathcal{R}_0^{(2)} = 0.7064 < 1$ and $\mathcal{R}_0^{(3)} = 0.3126 < 1$), $m_{32} = m_{23} = m_{13} = m_{31} = m_{12} = m_{21} = 0.2$. All other parameter values are as in Table 1

But the prevalence of the disease is larger in the patch with higher infectivity. Thus, the impact of the disease is more important than in Fig. 9.

5 Conclusion

In this paper, we presented a system of differential equations describing the TB spread in heterogeneous complex metapopulations. A more general demographic structure was incorporated into the model in comparison to the previously published articles [49]. The model included the difference in disease transmission among different patches and the difference between the dispersal rates of susceptible individual and infective individuals, which simulates the process of disease control. We divided the infective population into two major types: the diagnosed infected population with limited transmission rate (i.e. frequency-dependent or pseudo mass action); the second infectious type called "undiagnosed" infectious population with a non-limited transmission rate model with mass action.

Our study show how complex it is to take into account human movements in a TB model. More complex is the network and more difficult it will be to control the spreading of the disease. In fact, we say that our approach permit to sustain or to establish that local interventions can be benefit for the whole population. Mathematically the model is not very easy to handle, but we have been able to show some interesting results.

The basic reproduction number $\mathcal{R}_0$ was computed and we showed that the disease-free equilibrium is globally asymptotically stable when the basic reproduction number is less than the unity. Using implicit function theorem, it was shown that there exists a unique endemic equilibrium in a neighborhood of the isolated endemic equilibrium for weak (small) migration rates.

Through numerical simulations, some disease spread scenarios in three and fifteen patches was analyzed. The case

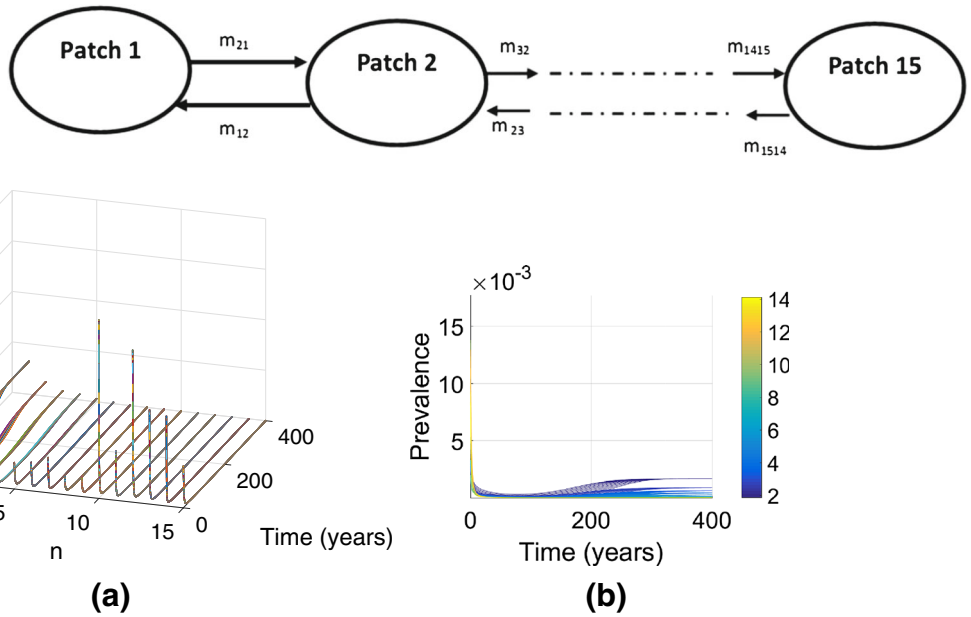

Fig. 8 Interaction between fifteen patches

Fig. 9 Prevalence of TB when $\eta = 1$ and $\beta_i \in (0.2, 0.71)$, $\pi_i \in (500; 1900)$ (so that $\mathcal{R}_0^{(1)} = 1.6589$, $\mathcal{R}_0^{(2)} = 0.6037$, $\mathcal{R}_0^{(3)} = 0.4673$, $\mathcal{R}_0^{(4)} = 0.9251$, $\mathcal{R}_0^{(5)} = 0.7725$, $\mathcal{R}_0^{(6)} = 0.7496$, $\mathcal{R}_0^{(7)} = 0.5587$, $\mathcal{R}_0^{(8)} = 0.6753$, $\mathcal{R}_0^{(9)} = 0.8468$, $\mathcal{R}_0^{(10)} = 0.4731$, $\mathcal{R}_0^{(11)} = 0.6268$, $\mathcal{R}_0^{(12)} = 0.1563$, $\mathcal{R}_0^{(13)} = 0.2728$, $\mathcal{R}_0^{(14)} = 0.7266$ and $\mathcal{R}_0^{(15)} = 0.8750$). All other parameter values are as in Table 1

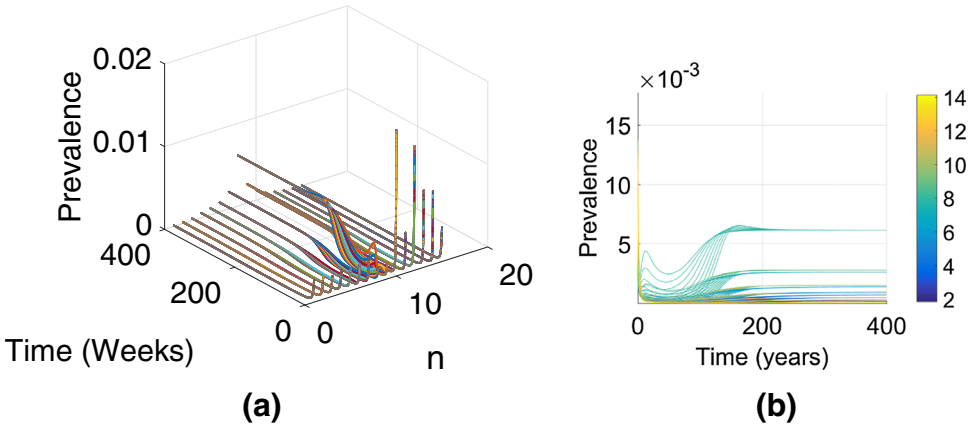

Fig. 10 Prevalence of TB when $\eta = 1$ and $\beta_i \in (0.2, 0.71)$, $\pi_i \in (500; 1900)$ (so that $\mathcal{R}_0^{(1)} = 0.7137$, $\mathcal{R}_0^{(2)} = 0.6037$, $\mathcal{R}_0^{(3)} = 0.4673$, $\mathcal{R}_0^{(4)} = 0.9251$, $\mathcal{R}_0^{(5)} = 0.7725$, $\mathcal{R}_0^{(6)} = 0.7496$, $\mathcal{R}_0^{(7)} = 0.5587$, $\mathcal{R}_0^{(8)} = 1.4878$, $\mathcal{R}_0^{(9)} = 0.8468$, $\mathcal{R}_0^{(10)} = 0.4731$, $\mathcal{R}_0^{(11)} = 0.6268$, $\mathcal{R}_0^{(12)} = 0.1563$, $\mathcal{R}_0^{(13)} = 0.2728$, $\mathcal{R}_0^{(14)} = 0.7266$, and $\mathcal{R}_0^{(15)} = 0.8750$). All other parameter values are as in Table 1

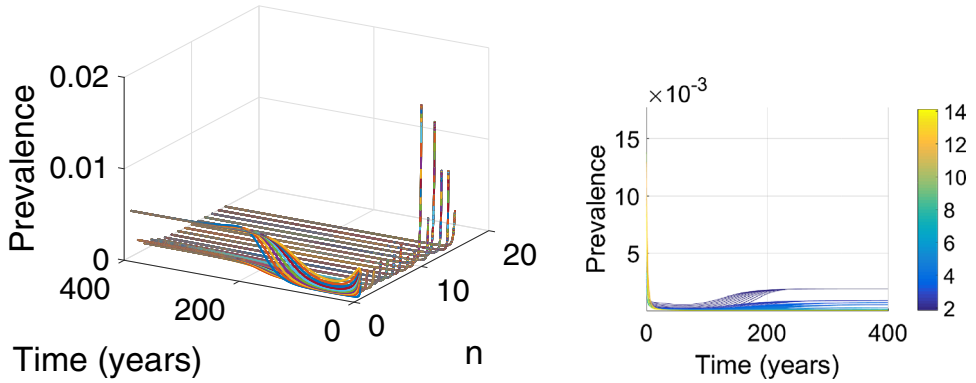

Fig. 11 Prevalence of TB when $\eta = 1$ and $\beta_i \in (0.2, 0.71)$, $\pi_i \in (500; 1900)$ (so that $\mathcal{R}_0^{(1)} = 1.6589$, $\mathcal{R}_0^{(2)} = 0.6037$, $\mathcal{R}_0^{(3)} = 0.4673$, $\mathcal{R}_0^{(4)} = 0.9251$, $\mathcal{R}_0^{(5)} = 0.7725$, $\mathcal{R}_0^{(6)} = 0.7496$, $\mathcal{R}_0^{(7)} = 0.5587$, $\mathcal{R}_0^{(8)} = 0.6753$, $\mathcal{R}_0^{(9)} = 0.8468$, $\mathcal{R}_0^{(10)} = 0.4731$, $\mathcal{R}_0^{(11)} = 0.6268$, $\mathcal{R}_0^{(12)} = 0.1563$, $\mathcal{R}_0^{(13)} = 0.2728$, $\mathcal{R}_0^{(14)} = 0.7266$, and $\mathcal{R}_0^{(15)} = 0.8750$). All other parameter values are as in Table 1

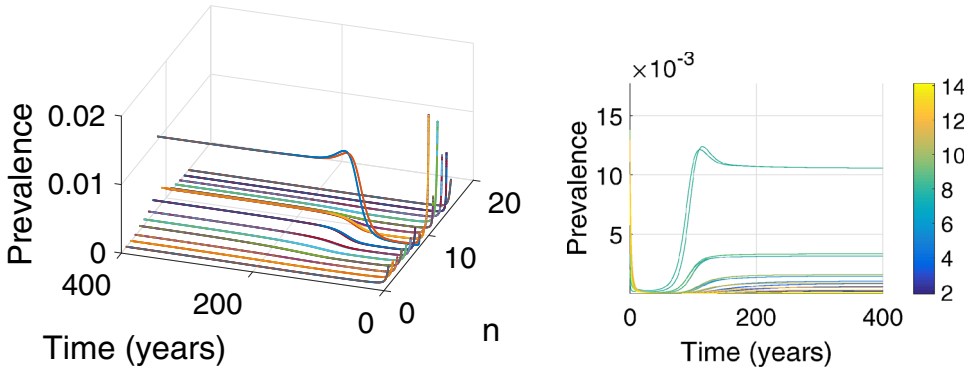

Fig. 12 Prevalence of TB when $\eta = 1$ and $\beta_i \in (0.2, 0.71)$, $\pi_i \in (500; 1900)$ (so that $\mathcal{R}_0^{(1)} = 0.7137$, $\mathcal{R}_0^{(2)} = 0.6037$, $\mathcal{R}_0^{(3)} = 0.4673$, $\mathcal{R}_0^{(4)} = 0.9251$, $\mathcal{R}_0^{(5)} = 0.7725$, $\mathcal{R}_0^{(6)} = 0.7496$, $\mathcal{R}_0^{(7)} = 0.5587$, $\mathcal{R}_0^{(8)} = 1.4878$, $\mathcal{R}_0^{(9)} = 0.8468$, $\mathcal{R}_0^{(10)} = 0.4731$, $\mathcal{R}_0^{(11)} = 0.6268$, $\mathcal{R}_0^{(12)} = 0.1563$, $\mathcal{R}_0^{(13)} = 0.2728$, $\mathcal{R}_0^{(14)} = 0.7266$, and $\mathcal{R}_0^{(15)} = 0.8750$). All other parameters values are as in Table 1

where the patches were connected two by two and different connection scenarios was analyzed and the spread of TB in neighbored patches was quantified depending on travel restriction scenarios. It was found that increasing the migration rate can help to better control the disease. In other word, increasing the number of person moving from patches with

high TB transmission to patches with better TB control might lead to a decrease of the overall cases. We also found that the disease propagation is function of the population size, and population size change speed of convergence to the disease free equilibrium when $\mathcal{R}_0 < 1$. Numerical simulation revealed that TB propagation in the patch with higher transmission rate was faster when the patch was not connected to other patches. The position of the patch with higher disease outbreak changes the number of infected in neighbors patches. Restriction on TB status for travelers was found to delay the propagation of the disease, but could not stop the disease if a better control was not applied in the patch with higher disease outbreak. The main difference was on the number of infectious in all patches. Also, when there is a travel restriction of infectious from patches with high prevalence to patches with low prevalence, the number of infective individuals in patches with high prevalence may increase when the migration rates decrease.

In the case of TB spread in 15 patches, TB might spread in closest four patches if TB is endemic in border patches, while TB will infect all patches if epidemic start from patch 8. We also showed that travel restriction will delay the propagation of the disease, and increase the number of infected in the affected patch.

In particular, through illustrative examples, we showed that the link between the values of the general basic reproduction number and local ones, which is really important from a practical point of view. Indeed, our illustrative examples indicate that the values of local basic reproductive numbers are of major importance not only to map the epidemiological risk in order to take into account where the risk of an epidemic is high, but to be able to indicates priority to lower some local basic reproduction numbers. Thus, among all cities where the risk is high, it seems important to make control in priority in cities where the Human population is large. In any case, each city has to make appropriate control campaign to lower the epidemiological risk. In the case where some cities, with the largest populations, may have for any reason a large value of the basic reproduction numbers, then the disease can spread quickly to the whole domain, even when η is small, according to the network.

For future works, it will be interesting to consider the global existence and stability of an endemic equilibrium of the model under the influence of population dispersal among patches. This appeared to be a challenging mathematical problem we could not address in this study. The same analysis could be considered in the model including backward bifurcation. The conclusions drawn in this work are valid for the set of parameters used, most of them was taken in the recent literature of TB. In the event of a new highly pathogenic TB strain, which might result in vastly different disease parameter values, our analytic results would hold, but numerical simulations should be done accordingly.

References

1. Global Fund to Fight AIDS, Tuberculosis, and Malaria (2006) Fighting tuberculosis. Geneva, Switzerland. Retrieved 9 Sept 2006, http://www.theglobalfund.org/en/about/tuberculosis/default.asp
2. World Health Organization (2009) Global tuberculosis control: surveillance, planning, financing. World Health Organization, Geneva
3. Dye C, William BG (2000) Criteria for the control of drug resistant tuberculosis. Proc Natl Acad Sci USA 97:8180–8185
4. Snider J, Rabiglione M, Kochi A (1994) Global burden of tuberculosis. In: Bloom BR (ed) Tuberculosis, pathogenis, protection and control. ASM Press, Washington, pp 47–59
5. Bloom BR (1994) Tuberculosis: pathogenesis, protection and control. ASM Press, Washington
6. Hethcote HW, Thieme HR (1985) Stability of the endemic equilibrium in epidemic models with subpopulations. Math Biosci 75:205–227
7. Lajmanovich A, Yorke JA (1976) A deterministic model for gonorrhea in a nonhomogeneous population. Math Biosci 28:221–236
8. Hethcote HW (2000) The mathematics of infectious diseases. SIAM Rev 42(4):599–653
9. Sattenspiel L, Dietz K (2000) A structured epidemic model incorporating geographic mobility among regions. Math Biosci 128:71–81
10. Chalvet-Monfray K, Artzrouni M, Gouteux JP, Auger P, Sabatier P (1998) A two patch model of Gambian sleeping sickness: application to vector control. Acta Biotheor 46(3):207–222
11. Arino J, van den Driessche P (2003) A multi-city epidemic model. Math Popul Stud 10:175–193
12. Wang W, Mulone G (2003) Threshold of disease transmission in a patch environment. J Math Anal Appl 285(1):321–335
13. Fromont E, Pontier D, Langlais M (2003) Disease propagation in connected host population with density-dependant dynamics: the case of the feline leukemia virus. J Theor Biol 223:465–467
14. Wang W, Zhao X-Q (2004) An epidemic model in a patchy environment. Math Biosci 190:97–106
15. Lloyd AL, Jansen V (2004) Spatiotemporal dynamics of epidemics: synchrony in metapopulation models. Math Biosci 188:1–16
16. Ruan S, Wang W, Levin SA (2006) The effect of global travel on the spread of SARS. Math Biosci Eng 3:205–218
17. Arino J, Jordan R, van den Driessche P (2005) Quarantine in a multi-species epidemic model with spatial dynamics. Math Biosci 206:46–60
18. Allen LJS, Bolker BM, Lou Y, Nevai AL (2007) Asymptotic profiles of the steady states for an SIS epidemic patch model. SIAM J Appl Math 67:1283–1309
19. Auger P, Kouokam E, Sallet G, Tchuente M, Tsanou B (2008) The Ross–Macdonald model in a patchy environment. Math Biosci 216:123–131
20. Smith HL (1995) Monotone dynamical systems. An introduction to the theory of competitive and cooperative systems, vol 41. AMS, Providence
21. Murphy BM, Singer BH, Kirschner D (2002) Comparing epidemic tuberculosis in demographically distinct populations. Math Biosci 180:161–185
22. Murphy BM, Singer BH, Kirschner D (2003) On the treatment of tuberculosis in hetergeneous populations. J Theor Biol 223:391–404
23. Castillo-Chavez C, Song B (2004) Dynamical models of tuberculosis and their applications. Math Biosci Eng 1:361–404
24. Bacaër N, Ouifki R, Pretorius C, Wood R, Williams B (2008) Modeling the joint epidemics of TB and HIV in a South African township. J Math Biol 57:557–593. doi:10.1007/s00285-008-0177-z

25. Bowong S, Tewa JJ (2009) Mathematical analysis of a tuberculosis model with differential infectivity. Commun Nonlinear Sci Numer Simul 14:4010–4021
26. Blower SM, Small PM, Hopwell PC (1996) Control strategies for tuberculosis epidemics: new models for old problems. Science 273:497–520
27. Castillo-Chavez C, Feng Z (1997) To treat or not to treat: the case of tuberculosis. J Math Biol 35:629–635
28. Cohen T, Colijn C, Finklea B, Murray M (2007) Exogenous re-infection and the dynamics of tuberculosis epidemics: local effects in a network model of transmission. J R Soc Interface 4:523–531
29. Bhunu CP, Mushayabasa S, Tchuenche JM (2011) A theoretical assessment of the effects of smoking on the transmission dynamics of tuberculosis. Bull Math Biol 3:333–357. doi:10.1007/s11538-010-9568-6
30. Golub GH, Van Loan CF (1996) Matrix computations. Johns Hopkins University Press, Baltimore
31. Anderson RM, May RM (1992) Infectious disease of humans, dynamical and control. Oxford University Press, Oxford
32. Anderson RM, May RM (1879) Population biology of infectious diseases: part I. Nature 280:361–367
33. Capasso V (1993) Mathematical structures of epidemic systems. Lecture notes in biomathematics, vol 97. Springer, Berlin
34. Moualeu DP, Weiser M, Ehrig R, Deuflhard P (2015) Optimal control for a tuberculosis model with undetected cases in Cameroon. Commun Nonlinear Sci Numer Simul 20(3):986–1003
35. Moualeu-Ngangue DP (2013) A mathematical tuberculosis model in Cameroon. PhD thesis, FU Berlin
36. Moualeu-Ngangue DP, Röblitz S, Ehrig R, Deuflhard P (2015) Parameter identification in a tuberculosis model for Cameroon. PLoS ONE 10(4):e0120607
37. Styblo K, Meijer J, Sutherland I (1969) The transmission of tubercle bacilli: its trend in a human population. Bull Int Union Tuberc 42:5–104
38. Berman A, Plemmons RJ (1994) Non-negative matrices in the mathematical sciences. Academic, New York
39. Jacquez JA, Simon CP (1993) Qualitative theory of compartmental systems. SIAM Rev 35:43–79
40. van den Driessche P, Watmough J (2002) Reproduction numbers and sub-threshold endemic equilibria for compartmental models of disease transmission. Math Biosci 180:29–48
41. Castillo-Chavez C, Thieme CHR (1995) Asymptotically autonomous epidemic models. In: Arino O et al (eds) Mathematical population dynamics: analysis of heterogeneity, vol 1. Theory of epidemics. Wuerz, Winnipeg, pp 33–50
42. Goursat E (1903) Sur la théorie des fonctions implicites. Bull Soc Math Fr 31:184–192
43. Danilov VI (2001) Implicit function (in algebraic geometry). In: Hazewinkel M (ed) Encyclopaedia of mathematics. Springer, Berlin
44. Kudryavtsev LD (2001) Implicit function. In: Hazewinkel M (ed) Encyclopaedia of mathematics. Springer, Berlin
45. Dushoff J, Huang W, Castillo-Chavez C (1998) Backwards bifurcations and catastrophe in simple models of fatal diseases. J Math Biol 36:227–248
46. Cohen T, Lipsitch M, Walensky RP, Murray M (2006) Beneficial and perverse effects of isoniazid preventive therapy for latent tuberculosis infection in HIV-tuberculosis co-infected populations. Proc Natl Acad Sci USA 103:7042–7047
47. National Institute of Statistics (2010) Evolution des systèmes statistiques nationaux, expérience du Cameroun. In: J. Tedou (ed) The National Institute of Statistics report, New-York, pp 1–18
48. National Comittee of Fight Against Tuberculosis (2010) Guide du personnel de la santé. In: Ministére de la Santé Publique (ed) The Ministry of Public Health report. CEPER Press, Yaoundé-Cameroon, pp 1–110
49. Hickson RI, Mercer GN, Lokuge KM (2012) A metapopulation model of tuberculosis transmission with a case study from high to low burden areas. PLoS ONE 7(4):e34411. doi:10.1371/journal.pone.0034411